UNIVERSITY POLITEHNICA OF BUCHAREST
Doctoral School of Materials Science and Engineering

Eng. Georgiana Claudia MILEA

Contributions in the field of biomaterials used and evaluation of the clinical functionality of metal implants for fracture repair

~ ABSTRACT~
PhD thesis

PhD supervisor:
Prof. Univ. Habil. Dr. Eng. ANTONIAC VASILE IULIAN

Bucharest 2022

UNIVERSITY POLITEHNICA OF BUCHAREST
Doctoral School of Materials Science and Engineering

~ ABSTRACT~
PhD thesis

Contribuții în domeniul biomaterialelor utilizate și a evaluării funcționalității clinice a implantelor metalice pentru repararea fracturilor

Contributions in the field of biomaterials used and evaluation of the clinical functionality of metal implants for fracture repair

PhD Student: Eng. MILEA GEORGIANA CLAUDIA
PhD supervisor: Prof. Univ. Habil. Dr. Eng. ANTONIAC VASILE IULIAN

Doctoral Commission

President	**Prof. dr. ing. Brandușa GHIBAN**	**University Politehnica of Bucharest**
PhD supervisor	**Prof. Univ. Habil. Dr. Eng. Vasile Iulian ANTONIAC**	**University Politehnica of Bucharest**
Scientific references	**Prof. Dr .eng. Petrică VIZUREANU**	**„Gheorghe Asachi" Tehnical University from Iaşi**
	Prof. Dr. Med. Marius NICULESCU	**Universitaty „Titu Maiorescu" Bucharest**
	Prof. Dr .Eng. Marian MICULESCU	**University Politehnica of Bucharest**

Bucharest 2022

INTRODUCTION

The objective of the present doctoral thesis of the doctoral thesis was to define and verify a protocol for the analysis of explants from the category of metal implants for osteosynthesis, made of austenitic stainless steel and titanium alloys, in order to establish their causes of failure, through associated use. of classical methods of investigation (stereomicroscopy, optical microscopy) with some modern methods of investigation (scanning electron microscopy associated with X-ray spectroscopy with energy dispersion, finite element analysis), as well as the implementation of verification of chemical composition and chemical homogeneity at the level of the metal implant by SDAR-OES spectrometry

The structure by chapters of the present doctoral thesis is presented in the following:

Chapter I entitled ***"Medical Clinical Aspects"*** brings together information from the literature on the skeletal system and its importance in the human body.

Chapter II entitled ***"The current state of implants for osteosynthesis"*** describes important aspects about damage to the bone system, bone fractures, the materials from which implants are made, but also the types of osteosynthesis implants used in medical practice.

Chapter III entitled ***"Experimentally used materials, methods and equipment"*** describes the experimental materials used, the work protocol followed in the case of the thesis and all the analysis techniques and equipment used for characterization.

Chapter IV entitled ***"Experimental results on the analysis of metal implants for osteosynthesis"*** presents the experimental results obtained from the activities of structural, morphological and compositional characterization of explants.

Chapter V entitled ***"Conclusions"*** is a final chapter in which the original conclusions and contributions are presented. Also, in this chapter are listed the personal contributions made during this research.

CHAPTER 1. MEDICAL CLINICAL ASPECTS

1.1. GENERAL CONSIDERATIONS

Bone is an extremely complex organ, which contains different types of tissue (blood, connective tissue, nerves, bone tissue) and represents 15% of body weight in newborns, 17% in adults up to 50 years and 14 % in the elderly [1]. This body has a resistance structure, adapted to the mechanics of the musculoskeletal system, but in permanent modeling and remodeling (renewal).

The major function of bones is to provide support, which allows the human body to maintain an upright position, as well as mechanical functions and protective function of vital structures such as the brain and intrathoracic organs.CAPITOLUL 2. STADIUL ACTUAL AL IMPLANTELOR PENTRU OSTEOSINTEZĂ

2.1. FUNDAMENTALS OF THE BONE PROTESION APPROACH

In terms of progress in the field of biomaterials, the aim is to increase human quality and longevity and thus to increase the effectiveness of biomaterials used [ISO 10993]. Therefore, any medical device used in implantology must comply with requirements regarding: proper design and manufacturability, biocompatibility, mechanical properties, wear resistance, corrosion resistance, osseointegration.

2.2. CURRENT STATE OF METAL BIOMATERIALS

2.2.1.1. The current state of stainless steels

The three main alloying elements in the most commonly used stainless steel (316L) are Cr, Ni and Mo. Cr alloying leads to the formation of a self-regenerating protective layer (passive layer of chromium oxide-Cr2O3) which is facilitated by immersion of the alloy in a concentrated solution of nitric acid. This passivating layer provides resistance to chemical attack and a high degree of electrical resistivity, thus ensuring very good protection against corrosion [1].

2.2.1.2. Current status of titanium and titanium alloys

Due to the excellent properties of titanium, namely the moderate modulus of elasticity (approx. 110GPa), good corrosion resistance and low density, titanium and titanium alloys are widely used as medical devices respectively artificial joints, bone fixators, spinal fixators, dental implant etc. [2-3]. Titanium has the following chemical and mechanical properties respectively: density equal to 4.5 g / cm3, mechanical strength (Rm), equal to 241Mpa for Ti of purity 99.175% and 550 MPa for Ti of purity 98.63%; elongation (Ti 99.175%) of 24%, high refractoriness, high corrosion resistance in aggressive environments [4].

2.2.1.3. The current state of magnesium alloys

Magnesium-based alloys have begun to attract the attention of researchers, so alloys such as Mg-8Al and Mg-4Al-0.3Mn have been investigated, in which slow degradation and the formation of a new callus have been observed, as well as the fact that Mg is complete. resorbable, non-toxic, has an anesthetic effect and it is also found that the formation of gas cavities associated with the implantation of Mg alloys has no negative effect on the body [5,6]. For the use of biodegradable implants in orthopedic applications to be possible, they must meet requirements regarding their properties / characteristics such as [7]: adequate mechanical strength, ductility, fatigue strength, biocorrosion resistance.

2.2.2 Types of implants for osteosynthesis

A fracture is a discontinuity in the bone axis caused by an overload, being unstable it requires osteosynthesis for temporary stabilization.

Screwed metal plate osteosynthesis aims to fix the fracture through a simple mechanical system as a principle, but which works asymmetrically on a heterogeneous bone substance as a mechanical structure and behavior. In the case of fractures located at the extremities, the monobloc plate-plate or blade-plate systems are used, introduced at the diaphyseal-epiphyseal junction, which ensure a good osteosynthesis of the epiphyseal fractures. Of the existing fastening systems of the nail-plate, blade-plate or screw-plate type, the ones that show favorable results are the screw-compression type (DKP, DHS- for the upper end of the femur, DCS- for the lower end of the femur).

For isolated osteosynthesis, screws are used to bring together bone fragments. There are basically two main categories of screws, namely those for the cortical bone (self-tapping screws and AO screw), and those for the spongy bone that have a wide-pitched helix-shaped thread.

CHAPTER 3 RESEARCH METHOD

3.1. The purpose of the doctoral thesis

The main purpose of the doctoral thesis was to define and verify a protocol for analyzing explants in the category of metal implants for osteosynthesis, made of austenitic stainless steel and titanium alloys, in order to establish their causes of failure, by the associated use of classical methods. (stereomicroscopy, optical microscopy) with some modern methods of investigation (scanning electron microscopy associated with energy dispersive X-ray spectroscopy, finite element analysis), as well as the implementation of chemical composition and chemical homogeneity verification at the metal implant by SDAR-OES spectrometry.

3.2. The objectives of the doctoral thesis

1. Definition and verification of a protocol for the analysis of metal implants for osteosynthesis in order to investigate and establish their causes of failure.
2. Application of the method for estimating the uncertainty of the measurement of elemental concentrations with SDAR-OES equipment to verify the chemical composition of the metallic material and the chemical homogeneity of the implant
3. Assessment of the chemical conformity of several implants such as metal implants for osteosynthesis
4. Establishment of the failure mechanism for a number of 7 different explants, such as metal implants for osteosynthesis, made of austenitic stainless steel and titanium alloys.
5. Highlighting some problems encountered in clinical practice regarding the use of screws for fixing osteosynthesis plates, being identified the phenomenon of corrosion in the crevasse, which in association with the micromovement of the screws leads to a faster rupture.
6. The associated use of classical methods of investigation (stereomicroscopy, optical microscopy) with some modern methods of investigation (scanning electron microscopy associated with X-ray spectroscopy with energy dispersion, finite element analysis) to establish the mechanisms of failure in the case metal implants for osteosynthesis, made of austenitic stainless steel and titanium alloys.

3.3 ESTABLISHMENT OF THE PROTOCOL FOR THE EXPLANATION OF MEDICAL DEVICES

In order to identify the causes that led to the failure of the implants, a protocol was established which was subsequently applied to the cases studied. The protocol for explanting medical devices is presented in table 3.1.

Table 3.1 Protocol for explanted medical devices

I. Clinical data	**Information obtained**	**Degree of importance ***
Patient record	Name, Surname, Age, Sex	
	Internal diagnosis	YEAR
	Clinical observation sheet (number)	PO
	Date and hospital where the implant was performed	N
	Date and hospital where the explant was performed	N
	The reason for exploding the medical device	YEAR
	Identification of the exploded device (type and components)	YEAR
	Medical device data (batch number, series, manufacturer)	December
	Remarks	December
Radiological images	Identification of broken components of the implant	YEAR
	View callus format	
Visual observation of prosthetic components	Possible organic deposits and identification of observed irregularities	N

II Data on biomaterial	**Information obtained**	**Degree of importance ***
Analysis of the design and biomaterials used	Correlations between implant design and type of medical condition	YEAR
	Identify the appropriate use according to the medical condition	YEAR
III Methods used to investigate the explant	**Information obtained**	**Degree of importance ***
Argon-spark excitation optical emission spectrometry (SDAR-OES)	Measurement of the elemental composition of biomaterial	YEAR
	Estimation of chemical homogeneity of biomaterial (Y / N *)	and
	Chemical conformity assessment of biomaterial (C / N *)	and
Macroscopic analysis by macrophotography and stereomicroscopy	Identify the rupture mechanisms that led to implant failure	and
	Observation of rupture surfaces and identification of the type of rupture	and
Optical microscopy tests	Identification of typical microstructural characteristics for the investigated alloy	N
	Identification of potential structural defects	and
Scanning and Elemental Analysis Electron Microscopy (SEM-EDS)	Measurement of the elemental composition in the areas of interest of the biomaterial	N
	Morphology of breaking surfaces In order to identify breaking mechanisms	and
	Identification of possible structural inhomogeneities (inclusions) in the rupture zone	and
Biomechanical analysis by FEA method (Finite element analysis)	Simulation on the distribution of alloy stresses depending on the type of implant	December
	Intercomparison of the results obtained in the simulation regarding the mechanical behavior of the bone and the implant	UEC

**Imperative; AN absolutely necessary; Necessary; DEC- if applicable; UEC where applicable; PO- can be omitted;*

Following the evaluation of a number of 20 explants were identified: 1 explant used for osteointegration of the clavicle, 6 explants used for osseointegration of the humerus bone, 7 explants used for osseointegration of the tibial bone, 6 explants used for osseointegration of the femur bone. The selection criterion of the 7 investigated explants was based on their use in the type of fractured bone and the type of material.

Table 3.2 shows the type of explant, the type of bone and the type of alloy used.

Table 3.2 Presentation of the investigated evidence in the thesis

Nr. crt.	The type of explant	Device data	Bone type _	Type alloy predicted	Sample code
1	Plate anatomical , with screws blocked for clavicle fractures _	C *	Clavicle	- plate - non- alloy titanium	**PS1**
				- unalloyed titanium screw	**PS1-screw**
2	Plate with screws type LCP for humerus fractures _	C *	humerus	- plate - non- alloy titanium - unalloyed titanium screw	**PS2**
3	Rod intramedullary Siedel	C *	humerus	Steel 316L stainless steel	**TCS3**
4	Rod intramedullary tibial	C *	tibia	Ti -6A-4V	**TCT4**
5	Rod intramedullary tibial titanium; Screw 4.5mm latch	C *	calf	Ti -6A-4V	**TCT5**
6	Rod centromedullary femur, universal	C *	Femur	Ti -6A-4V	**TCF6**

7	Rod centromedullary femur	C *	Femur	Steel 316L stainless steel	**TCF7**

*C * Data about the device that is known but cannot be mentioned nominally so as not to infringe the right to the protection of personal data!*
In the following will be presented the results of the investigations on the extracted implants (explant) that failed, applying the implemented protocol.

CHAPTER 4 EXPERIMENTAL RESULTS ON THE ANALYSIS OF METAL IMPLANT IMPLANTS FOR OSTEOSYNTHESIS

4.2. EXPERIMENTAL RESULTS

4.2.1. Sample PS1

4.2.1.1. Clinical data on the implanted patient

Table 4.1 Clinical data of the patient

PATIENT (*name, surname, age, sex*)	LA, 28; male
INTERNAL DIAGNOSIS	Clavicle fracture (right)
CLINICAL OBSERVATION SHEET (*number*)	-
DATE and HOSPITAL in which the ***implantation was performed***	Orthopedic Clinic 2, Colentina Clinical Hospital Bucharest
DATE and HOSPITAL in which the ***explant was performed***	Orthopedic Clinic 2, Colentina Clinical Hospital Bucharest
THE REASON FOR EXPLANING THE MEDICAL DEVICE	Rupture of the metal implant for osteosynthesis and clavicle fracture, 3 months after primary implantation
IDENTIFICATION OF THE EXPLANTED DEVICE (* *type and components*)	Anatomical plate with locked screws for clavicle fractures
DEVICE DATA (* *batch and device serial number, manufacturer)*	C*

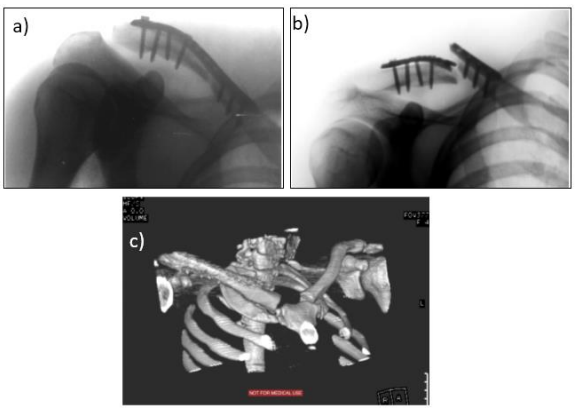

Fig. 4.2. X-ray images of the PS1 sample a) Before rupture (initial implantation), b) after rupture, c) CT image with 3D reconstruction pr-revision intervention (part of the operating protocol)

4.2.1.2. Investigations into chemical composition, chemical conformity and homogeneity assessment

4.2.1.2 a) Measurement of local chemical composition

The evaluation of the chemical homogeneity of the PS1 sample was performed at the level of the test piece (sample), at which level the chemical homogeneity test is considered to be of the "in-bottle" type. Thus, for the evaluation of chemical homogeneity, the t-Student statistical test was applied using the experimental standard deviation of the means.

The reporting of the obtained results was performed in accordance with the values of the concentrations of the elements specified in the standards ISO 5832-3: 2016 (in the case of the screw) and ISO 5832-2: 2018 (in the case of the plate). Following the application of the t-Student test, it was found that the PS1 test satisfies the homogeneity criteria for all the elements specified in the standard.

In the case of the PS1-screw sample, a sufficient number of measurements could not be performed to be able to apply the t-Student test in order to evaluate the chemical homogeneity due to its limited dimensions.

4.2.1.2 b) Chemical conformity assessment

The chemical conformity assessment was performed both in detail taking into account the results of measurements locally and globally (synthetically) using the mean of the averages ($\bar{\bar{c}}$) and the uncertainty of the mean of the averages ($U_{\bar{\bar{c}}}$). Thus, in the following will be presented the results obtained

Table 4.2. Overall results of the chemical conformity test (CC) corresponding to the PS1 sample

Element [%]	Fe	C	N
LS[1]	*max* 0.30	*max* 0.1	*max* 0.03
LI[2]	-	-	-
$\bar{\bar{c}}$	0.246	0.035	0.008
U [95%]	0.005	0.004	0.0025
LSB[3]	0.295	0.096	0.0275
LIB[3]	-	-	-
TCC[4]	**1**	**1**	**1**

1 Upper limit; 2 Lower limit; 3 Acceptance tape; 4 the result of the chemical conformity test

Following the assessment of the chemical conformity of the rod at local and global level, it can be stated based on the results obtained that Ti is compliant in terms of element concentrations and if the extended measurement uncertainties are taken into account (U [95%]) it can be stated that the alloy subjected to measurements corresponds to the predicted mark.

In the case of the PS1-screw sample, a global chemical conformity assessment was performed based on 5 measurements. Thus in table 4.17 the result of the chemical conformity test is represented. To verify the deviation of the SDAR-OES spectrometer, the certified reference material of MBH Analitycal LTD BS T-5A type was measured 10 times. The extended uncertainties (U) with a 95% confidence level associated with the concentration specified in the standard were calculated and the chemical conformity assessment test was performed.

Table 4. 3 . Overall results of the chemical compliance test (CC) - corresponding to the PS1 sample - screw

Element [%]	C	N	Fe	V	Al
LS[1**]	*max*0,08	*max* 0.05	*max* 0.30	4.5	6.75
LI[2**]	-	-		3.5	5.5
$\bar{c}$	0.011	0.007	0.146	4.01	5.99
U [95%]	0.001	0.0005	0.004	0.013	0.275

LSB[3]	0.079	0.049	0.296	4.487	6.475
LIB[3]	-	-	-	3.487	5.225
TCC[4]	1	1	1	1	1

After performing the chemical conformity test, it can be stated that the screw meets the conformity requirements with the brand specification.

In conclusion, for both test types PS1 and PS1-screw respectively the chemical compliance test reveals that they comply with the brand specification, therefore the non-conformity of the material can be eliminated as an influencing factor that would have led to the failure of the osseointegration plate.

4.2.1.3. Macroscopic analysis and microscopy tests (MO and SEM) to investigate the explant in terms of macrostructure, microstructure and morphology of the breaking surface

Figure 4.3 shows the macrograph of the implant used for osteosynthesis of the fracture in the right collarbone. To identify the type of rupture, the fracture surfaces were analyzed using the stereomicroscopy method (c, d). Experimental samples were taken from the exploded screw plate

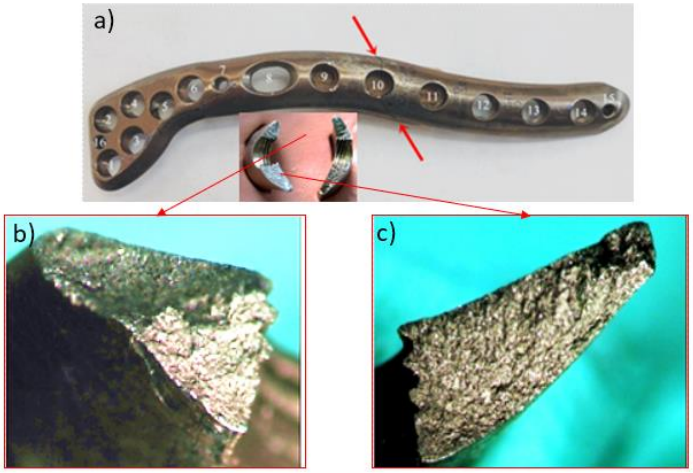

FIG. 4.3. Images of the breaking surface a) macrograph of the screw plate b, c) details of the breaking surface

Following the analysis of certified clinical data and the results obtained following the investigation by medical imaging, the fixing of the plate was performed by inserting 7 screws in holes 2, 3, 5, 6, 12, 13, 14. It can be seen in Figure 4.3 a) that the rupture of the plate occurred near the hole 10 and in the inserted image the breaking surface can be observed. Figure 4.3 b, c) shows details of the breaking surface which reveals the appearance of the breaking areas and implicitly the type of breaking and respectively fragile breaking.

Figure 4.4 shows optical microscopy images of the two resulting samples, respectively sample 1 in longitudinal section and sample 2, in cross section.

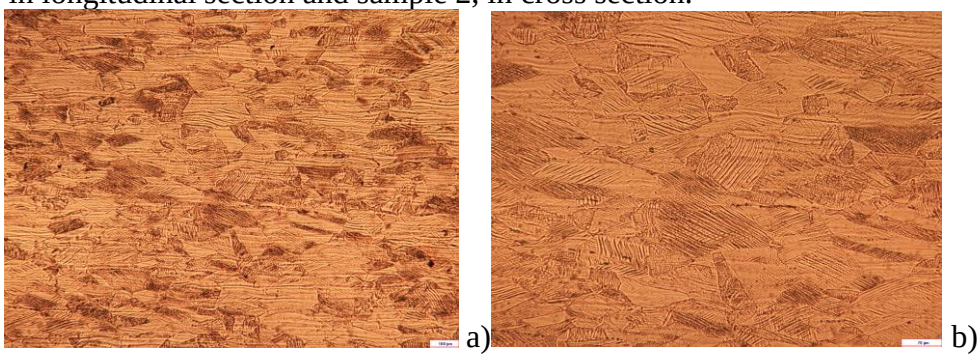

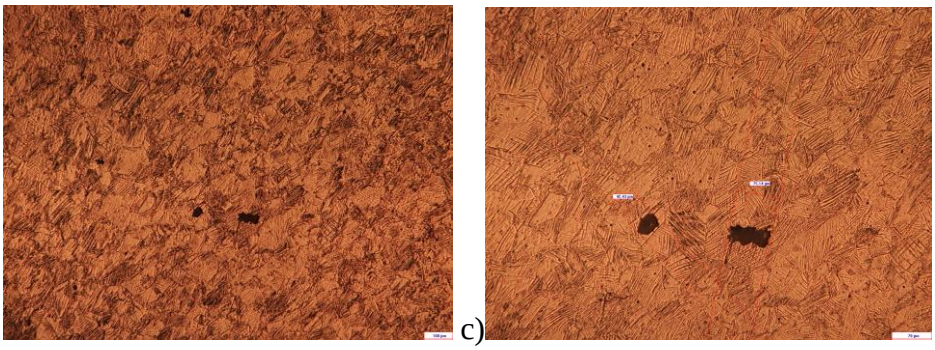

c) d)

FIG. 4.4. Optical microscopy images of samples 1 and 2 (PS1 sample); a, b) longitudinal section; c, d) cross section .

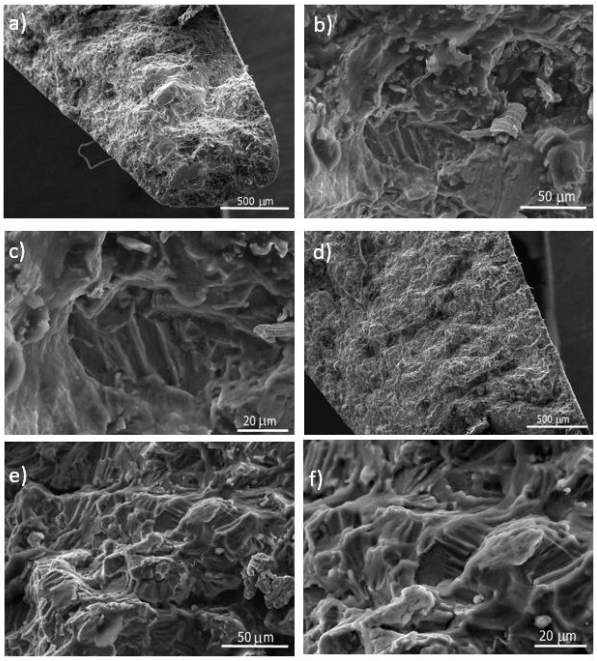

Fig 4.5. SEM images of the breaking surface a) morphology of the breaking surface of zone I, b) detail associated with figure a), c) detail associated with figure b); d) morphology of the breaking surface of zone II, e) detail associated with figure d), f) detail associated with figure e)

a. Screw 2, magnification 25x *b. Screw detail 2, 100x magnification*

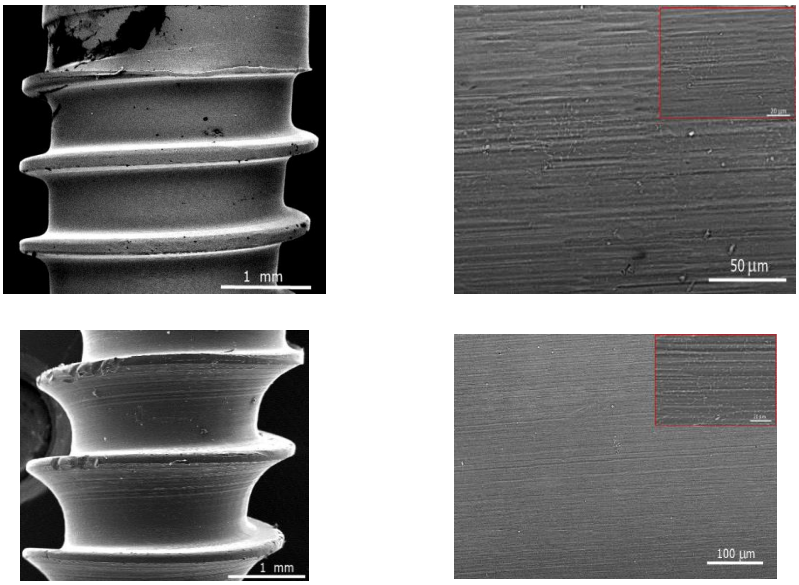

c. Screw 2, magnification 25x *d. Screw detail 2, magnification 100x*

Figure 4.6. SEM images of two screws a) screw 1 b) detail associated with figure a); c) screw 2 d) detail associated with figure d)

Following the SEM analysis it can be seen in figure 4.6 (a) the tendency of flattening of the helical rib of the screw 10 as a result of the force exerted by the plate following its rupture.

4.2.1.4. Finite element analysis

Due to the fact that the materials used in the case of osteosynthesis did not show material defects and the chemical composition complied with the material specifications, it was necessary to simulate the mechanical behavior of the stabilizing plate to identify possible causes that could have leads to implant failure. Thus, the simulation of the board behavior was performed by Ansys 12.0 finite element analysis. The default simulation model for the screw plate was used in the analysis program (figure 4.7).

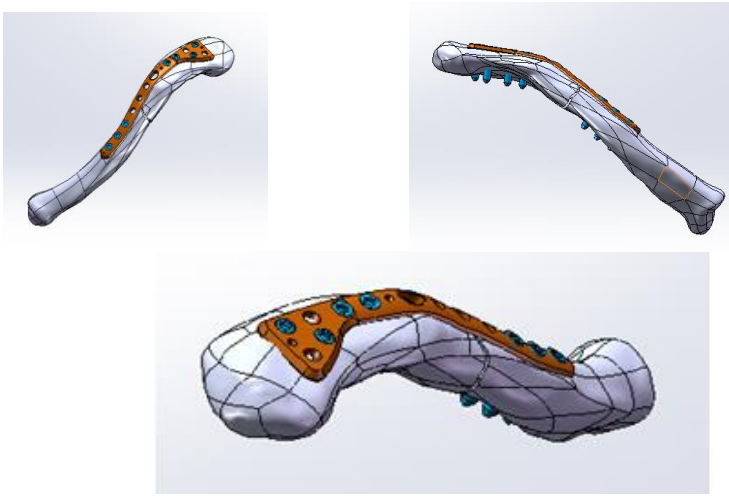

FIG. 4.7. Screw plate simulation model for humerus fractures

In order to identify the stresses acting on the clavicle stabilization plate when the assembly is subjected to certain loads, it was necessary to simulate two types of stresses.

For the FEA of the plate, the following conditions were selected, respectively: static structural analysis, division of the structure into finite elements (discretization of the structure) and tetrahedral elements with a size of 2 mm, establishing the contacts of the finite elements at their contour limits (figure 4.7 a, b) and the introduction of data on the chemical and physical properties of both the material and the bone.

Also, both analyzes use the same geometric pattern and loading scheme.

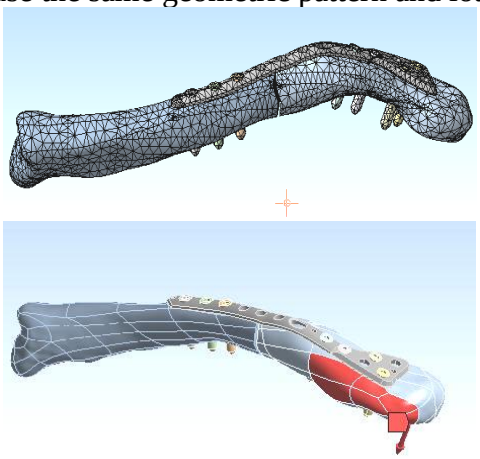

a) b)

Fig. 4.8 Representative image of the conditions established for the FEA a) Discretization of the structure - network characteristic of the whole; b) establishing the contour conditions

In the analysis of the FEA with the conditions corresponding to request I, two aspects were identified:
- the tension distribution follows the fracture direction of the bone
- by loading the collarbone in the direction of the anterior deltoid by more than 150 N, the stress values exceed the material flow limit. In this case, the phenomenon of material rupture can occur by initiating and propagating cracks that result in plate failure.

For the second type of stress (request II) the analysis of the simulation of the behavior of the screw plate was performed in the same way as in the case of the first type of stress, with the difference that in this case the application of forces will be located in another area . Figure 4.9 shows the result of the simulation and the total distribution of the equivalent elastic stress (Von Mises) at a load of 300 N following the activation of the pectoralis major.

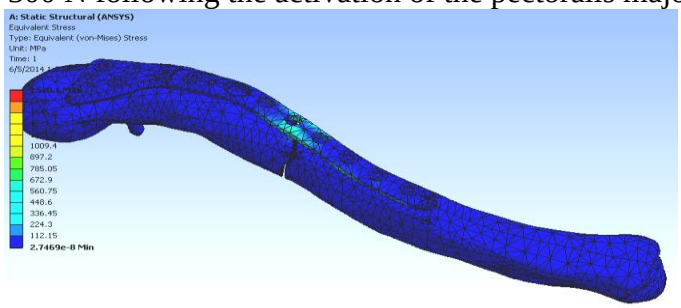

Fig. 4.9. Representative image of voltage distribution (Von Mises equivalent) at a load of 300N

4.2.2 PS2 test

4.2.2.1. Clinical data on the implanted patient

Table 4.4 presents the patient's clinical data, and Figure 4.14 shows images of bone fracture obtained by conventional radiology.

Table.4.4 Clinical patient data

PATIENT (*name, surname, age, sex*)	XX, 62 years old; male
INTERNAL DIAGNOSIS	Transverse humerus fracture - consolidation delay after orthopedic treatment
CLINICAL OBSERVATION SHEET (*number*)	-
DATE and HOSPITAL in which the ***implantation was performed***	Orthopedic Clinic 2, Colentina Clinical Hospital Bucharest
DATE and HOSPITAL in which the ***explant was performed***	Orthopedic Clinic 2, Colentina Clinical Hospital Bucharest
THE REASON FOR EXPLANING THE MEDICAL DEVICE	Rupture of the metal implant of osteosynthesis and pseudoarthrosis of the humerus, 2 months after a second fracture
IDENTIFICATION OF THE EXPLANTED DEVICE (* *type and components*)	LCP screw plate for humerus fractures

DEVICE DATA (* *batch and device serial number, manufacturer)*	**C***
REMARKS	The patient was advised to follow a standard postoperative program with immobilization for the first three weeks, followed by three weeks of passive movement and a period of active movement thereafter.

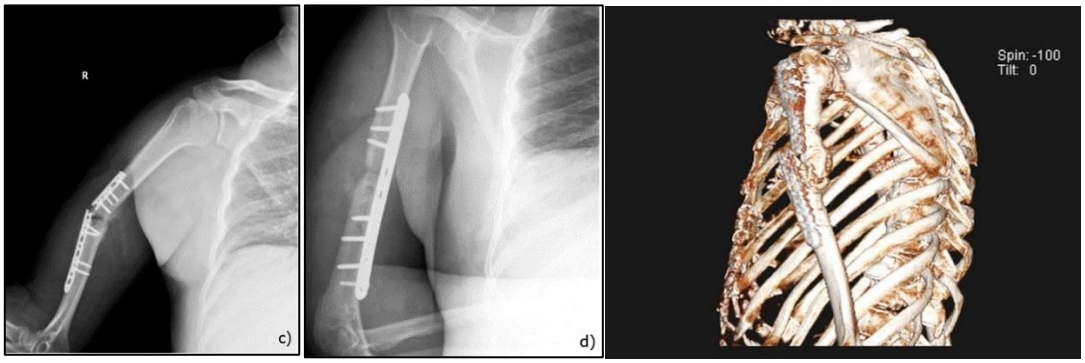

FIG. 4.10. X-ray images a) of the fractured bone, b) of the screw plate - initial implantation, c) of the screw plate after rupture, d) after revision with LCP Synthes type plate and autograft in focus of pesudarthrosis, e) CT image with 3D reconstruction [153]

4.2.2.2. Investigations into: determination of chemical composition, assessment of chemical conformity and estimation of compositional homogeneity

4.2.2.2 a) Measurement of local chemical composition

The evaluation of the chemical homogeneity of the exploded LCP type plate was performed at the level of the test piece (sample), at which level the chemical homogeneity test is considered to be of the "in-bottle" type. Thus, for the evaluation of chemical homogeneity, the t-Student statistical test was applied using the experimental standard deviation of the means.

The reporting of the obtained results was performed in accordance with the values of the concentrations of the elements specified in the ISO 5832-2 standard [150].

Following the application of the t-Student test, it was found that the PS2 test satisfies the homogeneity criteria for all the elements specified in the standard.

4.2.2.2 b) Chemical conformity assessment

The chemical conformity assessment was performed both in detail taking into account the results of the measurements locally and globally (synthetically) using the mean of the averages ($\bar{\bar{c}}$)and the uncertainty of the mean of the averages) ($U_{\bar{\bar{c}}}$).

Table 4.5 . Overall results of the chemical compliance test (CC) corresponding to the PS2 sample

Item [%]	Fe	C	N
LS [1]	*max*0.30	*max*0.1	*max* 0.03
LI [2]	-	-	-
$\bar{\bar{c}}$	0.269	0.034	0.018
U [95%]	0.005	0.004	0.0026
LSB [3]	0.295	0.096	0.0274
LIB [3]	-	-	-
TCC [4]	**1**	**1**	**1**

1 Upper limit; 2 Lower limit; 3 Acceptance tape; 4 the result of the chemical conformity test

Following the assessment of the chemical conformity of the plate locally and globally, it can be stated based on the results obtained that Ti cp Gr2 is compliant in terms of element

concentrations and if the extended measurement uncertainties are taken into account (U (95%)) stated that the alloy being measured **corresponds** the envisaged brand.

4.2.2.3. Macroscopic analysis and microscopy tests (MO and SEM) to investigate the explant in terms of macrostructure, microstructure and morphology of the breaking surface

From the point of view of the general appearance of the implant surface, it can be seen that it shows pronounced marks of scratching around the rupture area of the implant (figure 4.11). These traces are due to the process of implant recovery performed with surgical devices. At the macroscopic level, no specific corrosion characteristics were identified.

FIG. 4.11 Macrography of the LCP type explant

It can also be seen in Figure 4.11 that the rupture of the implant at the 6th hole at the near end of the humerus occurred, apparently in a straight line, but which forms an angle of 76 degrees in relation to the longitudinal axis of the plate. On the right, respectively 65 degrees on the left [153].

Fractographic investigation of rupture surfaces reveals that the surfaces have specific characteristics of adhesive wear (Figure 4.12 ae). The surfaces have been in contact under compressive forces for a long time.

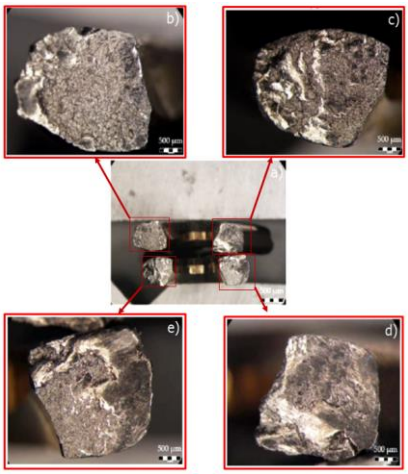

Fig. 4.12 Images of the breaking surface a) fractographic of the entire breaking area; be) details of the breaking surface [153]

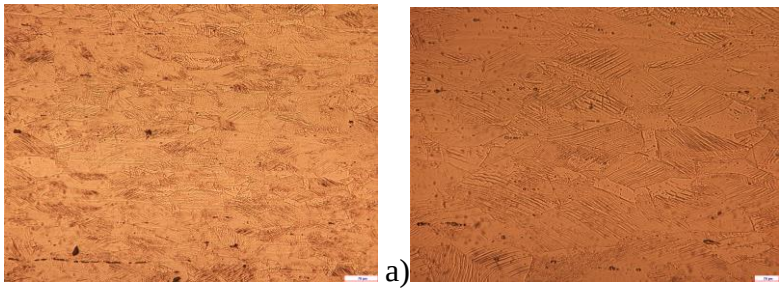

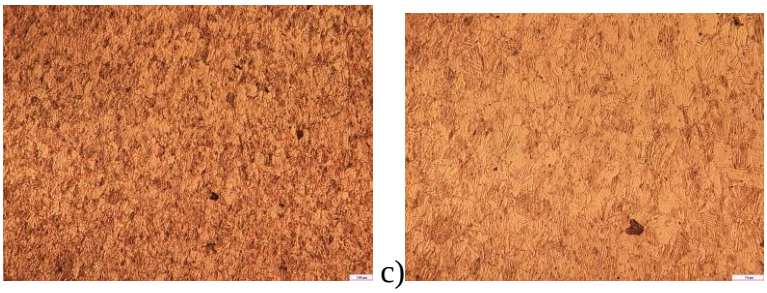

c) d)

FIG. 4.13. Optical microscopy images of samples 1 and 2 (PS2 sample); a, b) longitudinal section; c, d) cross section.

Figure 4.13 shows a microstructure characteristic of cp titanium with grains deformed according to the direction of flow of the material, the macles within each grain being proportional to the level of residual stresses. The grain size can be observed in cross section, this being approximated to an equivalent diameter of approx. 35 ÷ 50 microns. It is also observed the presence of inclusions of size comparable to that of grains.

In order to substantiate the phenomena / modes of rupture that took place in the case of the LCP type explant, investigations were performed in the area of its rupture using the SEM method. EDS analyzes were also performed to determine the chemical composition.

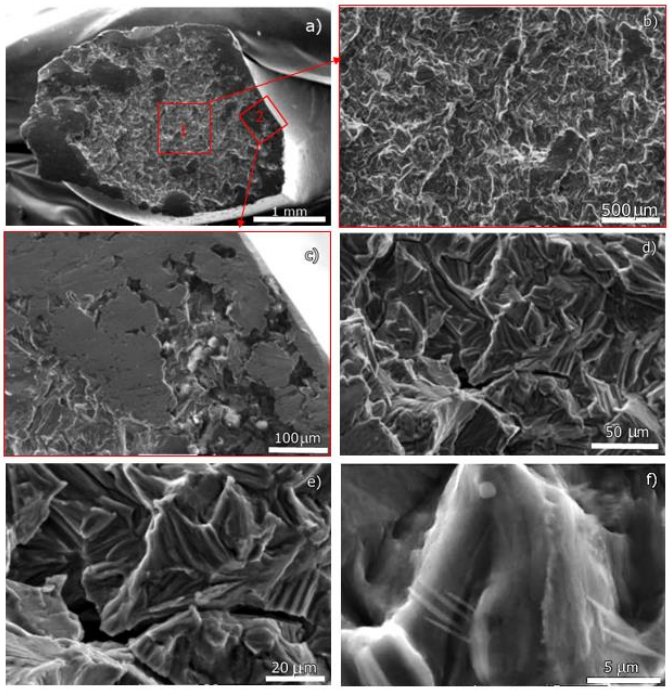

FIG. 4.14 SEM images of the breaking surface a) overview of the breaking surface b) detail associated with figure a) -area 1; c) detail associated with figure a) -zone 2; d) detail associated with figure c); e) detail associated with figure d); f) detail associated with figure e)

The images in figure 4.14 e, f show morphological aspects specific to the cleavage, in the direction of the local fissure. The second representative breaking surface is shown in figure 4.14 a). This surface corresponds to the part that gave way first and it can be seen that it has on its entire surface morphological aspects specific to wear. It is also noted that it has non-uniformity of the contour of the piece similar to the surface presented above [153].

4.2.2.4. Finite element analysis

In order to investigate the influence of the stress mode of the humerus on the implanted stabilization plate, the construction of the geometric model was performed by entering the data of the respective materials of the Ti and bone properties (table 4.36) and going through 3 stages.

The steps that have been taken for the construction of the geometric model are:

a) reconstruction of the humeral bone shown in the CT image, using the Mimics software

b) design of mechanical elements: plate and screws, using the SolidWorks 2013 computer-aided design program

c) assembly constraints and geometric constraints

Figure 4.15 shows: the division of the structure into finite elements (discretization of the structure) on the established model (*163485 elements, 94234 nodes)*, the established loads and restrictions (fixed support point (A) flexion muscles (B and D), abduction muscles (E and F), rotation muscles e (C) and joint reaction (G)), establishing the contacts of the finite elements between the parties involved (figure 4.15 c, d, e), for use in simulation (Ansys 13) .

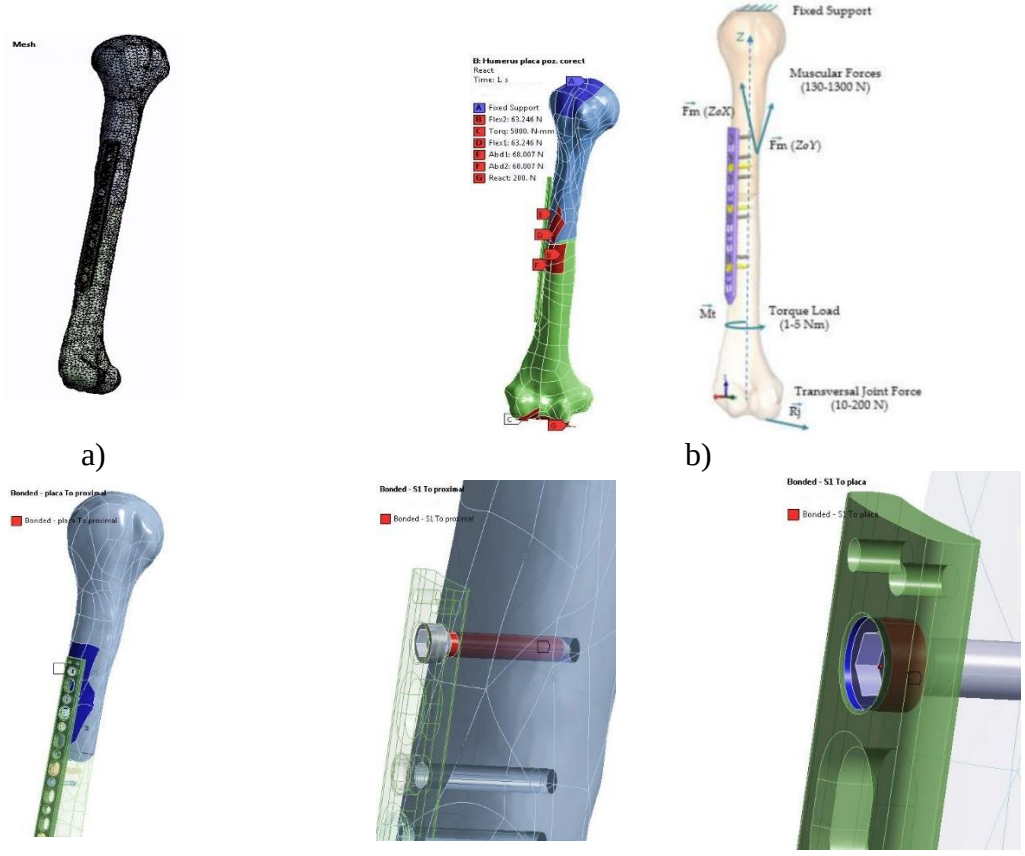

Figure 4.15 shows: the division of the structure into finite elements (discretization of the structure) on the established model (163485 elements, 94234 nodes), the established loads and restrictions (fixed support point (A) flexion muscles (B and D), abduction muscles (E and F), rotation muscles e (C) and joint reaction (G)), establishing the contacts of the finite elements between the parties involved (figure 4.15 c, d, e), for use in simulation (Ansys 13)

Loading scenario I. It refers to the stresses that appear in the plate when the subject tries to flex the humerus, using the deltoid muscle, while at the level of the palm act discreetly the weights of 1, 3, 5, 8 and 10 Kg.

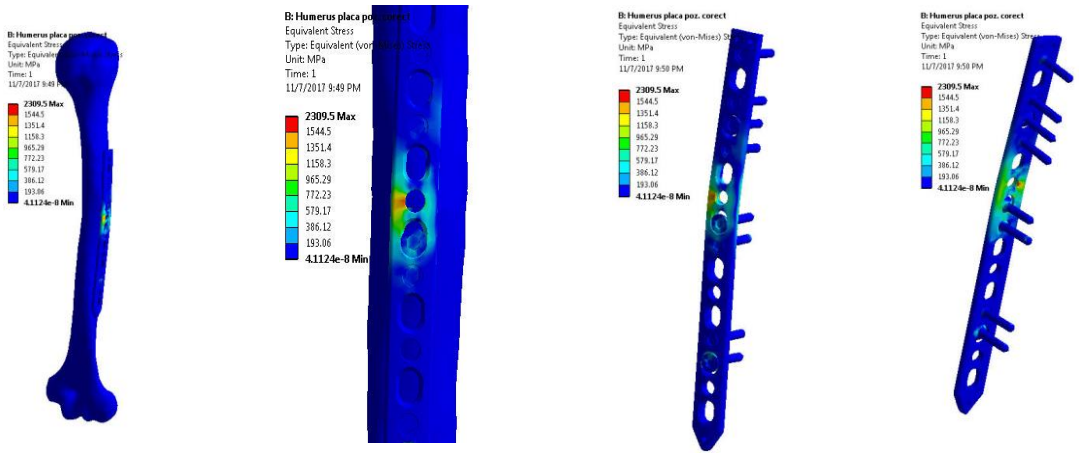

Fig. 4.16 Equivalent voltage distribution in the board: a) bone-plate overview; b) bone plate detail (side view) associated with figure a); c) overview of the plate with screws (front side view); d) overview of the screw plate (rear side view)

The second loading scenario refers to the demands that appear in the plate when the subject tries to achieve humerus abduction, while at the level of the palm the same weights act discreetly as in the case of the first scenario. Figure 4.17 shows the distribution of equivalent von Mises stresses in the LCP plate when it lifts a mass of 10 K

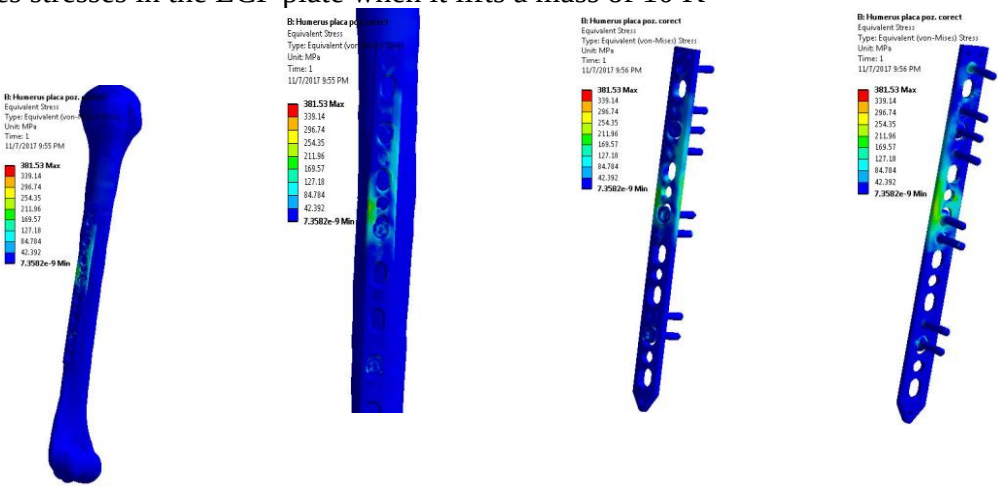

Fig. 4.17 Equivalent voltage distribution in the board: a) bone-plate overview; b) bone plate detail (side view); c) overview of the plate with screws (front side view); d) overview of the screw plate (rear side view)

The third scenario simulates the rotation trend achieved at the level of the rotator cuff and the deltoid. The values used in this case are torque and not force. The level of torsional stress was considered constant along the entire kinetic chain, and applied around the Z axis. Figure 4.18 shows the distribution of von Mises equivalent voltages in the LCP plate [153].

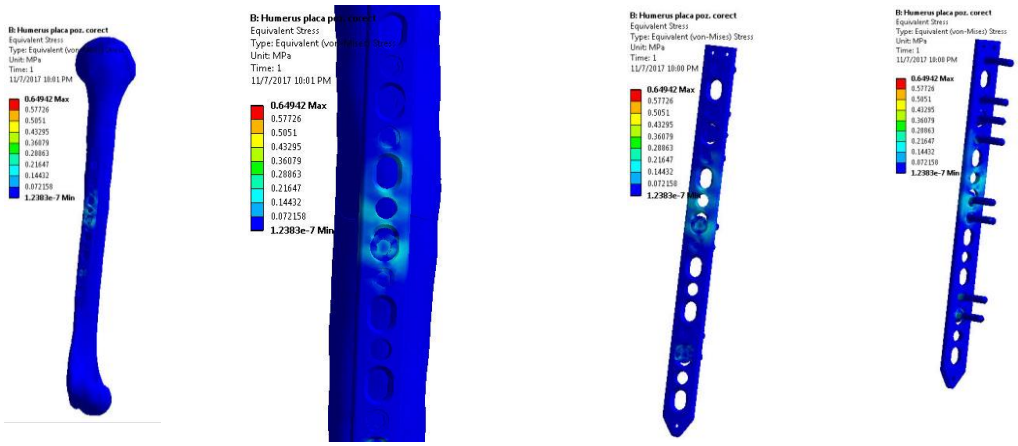

Fig. 4.18 Distribution of equivalent voltage in the board when applying a torque of 5Nm: a) plate-bone overview; b) bone plate detail (side view); c) overview of the plate with screws (front side view); d) overview of the screw plate (rear side view)

The last scenario (**IV**) simulates an action of pulling or pushing with the hand of an object that generates in the elbow joint a reaction of 10, 30, 50, 100 and 200 N and that has a direction perpendicular to the longitudinal axis of the humerus. In this case it is observed that above the value of 100 N, the stresses in the plate in the critical area exceed the breaking limit

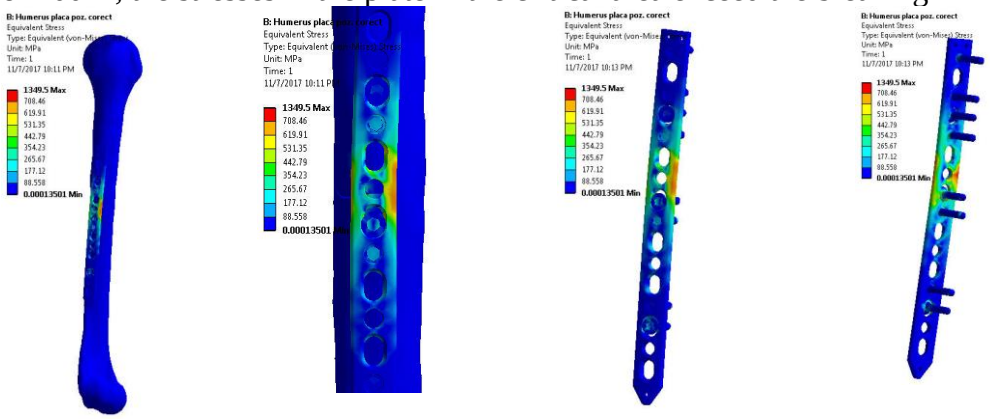

Fig. 4.19 Equivalent voltage distribution in the board: a) bone-plate overview; b) bone plate detail (side view); c) overview of the plate with screws (front side view); d) overview of the screw plate (rear side view)

TCS3 test

4.2.2.1. Clinical data on the implanted patient

4.2.3.1. Clinical data on the implanted patient

Table 4.7 presents the clinical data of the patient according to the established protocol, and Figure 4.20 presents images of bone fracture obtained by conventional radiology.

Table 4.7 Clinical data of the patient

PATIENT (*name* , *surname* , *age* , *sex*)	S. LA , 64, F.
INTERNAL DIAGNOSIS	Status after right humerus fracture operated in the 8 years ago . Pseudoarthrosis right humerus . Osteosynthesis material damaged .

CLINICAL OBSERVATION SHEET (*number*)	1334
DATE and HOSPITAL in which it was performed implantation	2005; another service
DATE and HOSPITAL in which it was performed explantation	2013, SCUB Floreasca
REASON FOR EXPLANING THE MEDICAL DEVICE	Pseudoarthrosis with damage osteosynthesis material _
IDENTIFICATION OF THE EXPLANTED DEVICE (* *type and component*)	Rod Seidel centromedullary ; Screw latching proximal 4.5mm; Screw expansion .

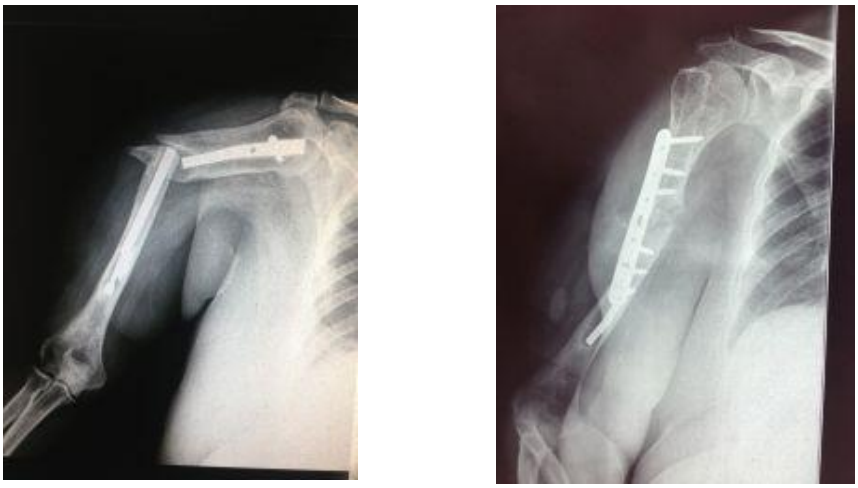

a) **b)**

FIG. 4.2 0 CT images of the plate with screws a) after rupture b) after îeplacement of the osteosynthesis implant

4.2.3.2. Investigations into: determination of chemical composition, assessment of chemical conformity and estimation of compositional homogeneity

4.2.3.2 a) Measurement of local chemical composition

The estimation of the chemical homogeneity of the exploded centromedullary rod was performed at the level of the test piece (sample), level at which the chemical homogeneity test is considered to be of the "in-bottle" type. Thus, for the evaluation of chemical homogeneity, the t-Student statistical test was applied using the experimental standard deviation of the means.

4.2.3.2 b) Chemical conformity assessment

The chemical conformity assessment was performed both in detail taking into account the results of measurements locally and globally (synthetically) using the mean of the averages ($\bar{\bar{c}}$)and the uncertainty of the mean of the averages $U_{\bar{\bar{c}}}$).

Table 4.8 . Global chemical compliance (CC) test results

Item [%]	C	And	min	P	S	-R	us	Mo	N	With
LS [1]	max 0.030	max 1.0	max 2.0	max0.025	max0.1	19	15	3.5	max 0.1	max 0.5
LI [2]	-	-	-	-	-	17	13	2.25	-	-
$\bar{C}_m$	0.024	0.421	1.76	0.013	0.004	17.21	14.15	2.77	0.093	0.086
U [95%]	0.002	0.03	0.01	0.003	0.001	0.1	0.01	0.02	0.01	0.01
LSB [3]	0.028	0.97	1.99	0.022	0.009	18.9	14.99	3.48	0.99	0.49

LIB [3]	-	-	-	-	-	17.1	13.1	2.29	-	-
TCC [4]	1	1	1	1	1	1	1	1	1	1

1 Upper limit; 2 Lower limit; 3 Acceptance tape; 4 the result of the chemical conformity test

Following the evaluation of the chemical homogeneity, the elements C and Si do not satisfy the homogeneity conditions. However, it can be seen that they meet the requirements for compliance with the brand specification.

Following the evaluation of the chemical conformity of the rod at local and global level, it can be stated based on the results obtained that the TCS3 sample **is compliant** Regarding the concentrations of the elements and if the extended measurement uncertainties (U [95%]) are taken into account, it falls within the specified limits.

In conclusion, the rod subjected to the measurement **corresponds to** the predicted mark, respectively 316L.

4.2.3.3. Macroscopic analysis and microscopy tests (MO and SEM-EDS) to investigate the explant in terms of macrostructure, microstructure and morphology of the fracture surface

Following macroscopic investigations it is observed that the rupture occurred in half _ _ proximal to the stem and the surface of the implant shows pronounced scratches of scratch around the area of rupture of the implant (figure 4.21). These traces are due to the process of implant recovery performed with surgical devices [154].

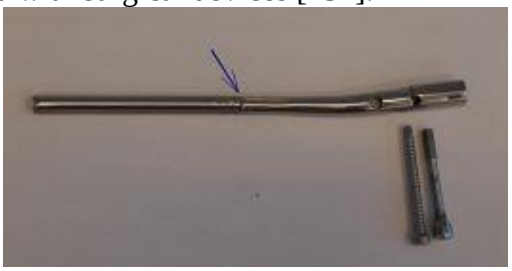

FIG. 4.34 Macroscopic image of the Siedel centromedullary rod showing the area of rupture

Figure 4.21 shows stereomicroscopy images taken on the rupture surface of the two components that form the centromedullary Siedel rod.

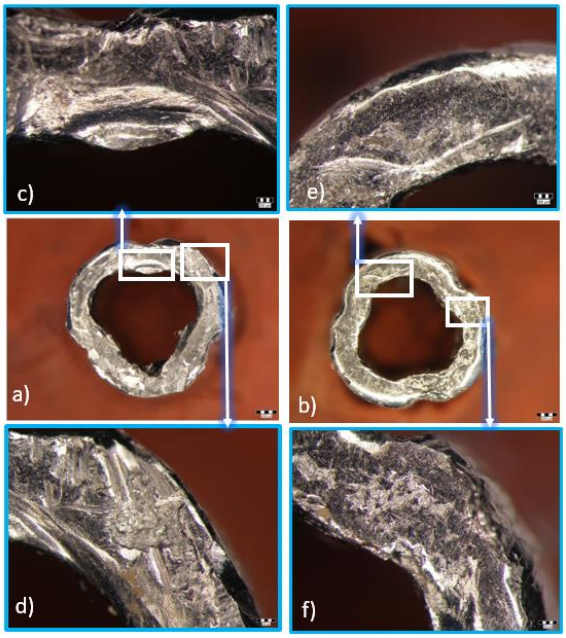

FIG. 4. 22. Images of the breaking surface of the two parts of the rod a) fractographic of the entire breaking area; b, e) details of the breaking surfaces; c, d) surface details associated with the areas in figure b); f, g) surface details associated with the areas in figure e) [154]

Figure 4.22a, b) shows the global breaking surfaces of the two rod components.

Figure 4.23 shows optical microscopy images of the resulting sample.

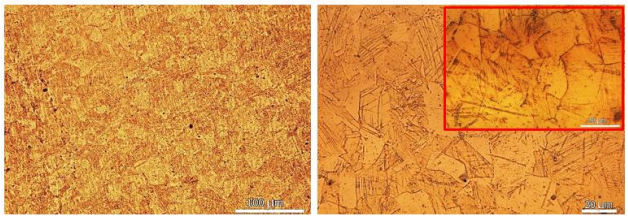

FIG. 4.23. Optical microscopy images corresponding to the TCS3 sample

Figure 4.23 shows a typical structure of stainless austenitic steel, respectively the solid austenite solution.

In the overall image corresponding to an area of the breaking surface of the rod (figure 4.24 a) it is observed that the surface has a smooth appearance typical for the phenomenon of crack propagation during material fatigue but at the same time shows a region where its own rupture occurred (final) and which presents different morphological aspects.

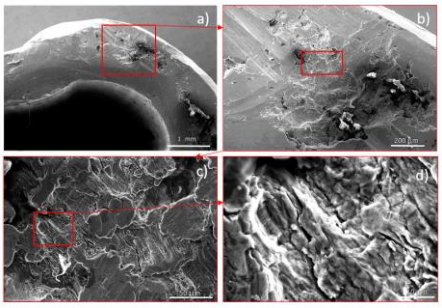

FIG. 4.24 SEM images of the breaking surface a) overview of a portion of the rod b) detail associated with figure a); c) detail associated with the area marked in figure b); d) associated with the area marked in figure b)

Figure 4.24 b shows traces caused by the instrument used by the doctor during the implant removal maneuver. It is observed that the cracks at the microscopic level are oriented in the same direction respectively NV-SE and extend on different planes with branch-type distribution as shown in Figure 4.24 d).

making stereomicroscopy analyzes , microscopy _ optical and microscopy scanning electronics have eliminated _ training imperfections _ and materials processing _ Right causes of rupture . Lack inclusion in the breaking zone or some _ POTENTIAL FAULTS structure is proof _ that the material from which it was made accomplished the implant does not constitute the cause of its rupture .

After an analysis careful data _ clinical , rupture rod intramedullary can be attributed breakage due to fatigue _ wear and tear to which it was subject in the the 8 years he was implanted .

In conclusion, the rupture was caused by the wear of the material over time.

4.2.4 TCT4 test

4.2.4.1. Clinical data on the implanted patient

Table 4.9 presents the patient's clinical data according to the established protocol, and Figure 4.25 presents images of bone fracture obtained by conventional radiology.

Table 4.9 Clinical patient data

PATIENT (*name, surname, age, sex*)	BM 43 years old, M.
INTERNAL DIAGNOSIS	Consolidation delay _ fracture tibial distance right operated Osteosynthesis material damaged .
CLINICAL OBSERVATION SHEET (*number*)	-
DATE and HOSPITAL in which the ***implantation was performed***	2017; another service
DATE and HOSPITAL in which the ***explant was performed***	2017, SCUB Floreasca
THE REASON FOR EXPLANING THE MEDICAL DEVICE	consolidation partial of a break cominutive with deterioration osteosynthesis material - rod _ locked
IDENTIFICATION OF THE EXPLANTED DEVICE (* *type and components*)	Rod intramedullary tibial
DEVICE DATA (* *batch and device serial number, manufacturer)*	**C***
REMARKS	Locking component distal with 3 screws - of which 2 distal were stable but mobility submitted through outbreak of the proximal led to rupture rod level _ a from locking holes _

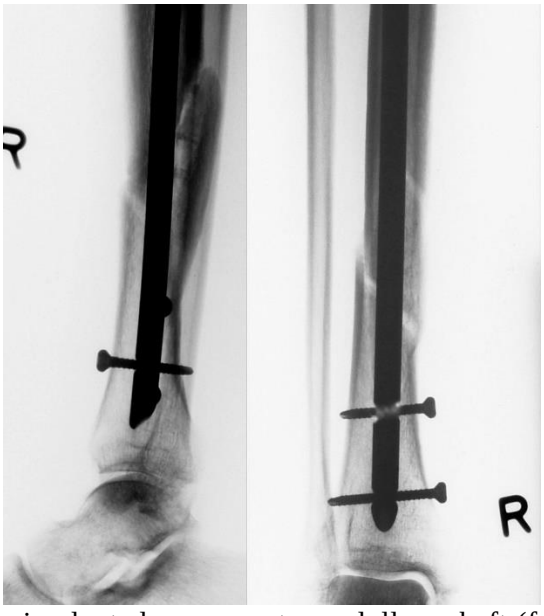

FIG. 4.25. X-rays of the implanted area - centromedullary shaft (front + profile 1/3 distal leg with implant in situ)

4.2.4.2. Investigations into: determination of chemical composition, assessment of chemical conformity and estimation of compositional homogeneity

4.2.4.2.a) Measurement of local chemical composition

The reporting of the obtained results was performed in accordance with the values of the concentrations of the elements specified in the ISO 5832-3: 2016 standard [151].

Following the application of the t-Student test, it was found that the sample satisfies the homogeneity criteria for all identified elements, respectively C, Al, Cr, Mo, Fe, Si, Sn.

4.2.4.2.b) Chemical conformity assessment

The chemical conformity assessment was performed both in detail taking into account the results of the measurements locally and globally (synthetically) using the mean of the averages ($\bar{\bar{c}}$)and the uncertainty of the mean of the averages) ($U_{\bar{\bar{c}}}$).

Table 4.10 . Overall results of the chemical conformity test (CC) corresponding to the TCT4 sample

Item [%]	C	N	Fe	V	the	-R	Mo	Sn	And
LS [1] **	*max*0.08	*max*0.05	*max*0.30	4.5	6.75	-	-	-	-
LI [2] **	-	-	-	3.5	5.5	-	-	-	-
$\bar{\bar{c}}$	0.039	-	0.331	-	6.35	**1.90**	**2.52**	**0.96**	**0.295**
U [95%]	0.002	-	0.01	-	0.027	**0.024**	**0.03**	**0.03**	**0.020**
LSB [3]	0.078	-	0.29	-	6.72	-	-	-	-
LIB [3]	-	-	-	-	5.47	-	-	-	-
TCC [4]	**1**	**1**	**0**	**0**	**1**				

1 Upper limit; 2 Lower limit; 3 Acceptance tape; 4 the result of the chemical conformity test

Following the assessment of the chemical conformity of the rod at local and global level, it can be stated based on the results obtained that the alloy **is not compliant .** Regarding the concentrations of the elements as shown in table 4.76. Thus, the alloy subject to measurement does not correspond to the predicted mark respectively Ti-6Al-4V [151]. Also, it was not possible to identify a type of biocompatible alloy that was similar to the investigated alloy. This may justify the improper behavior of the implant and is an obvious case of **malpractice** !

4.2.4.3. Macroscopic analysis and microscopy tests (MO and SEM) to investigate the explant in terms of macrostructure, microstructure and morphology of the breaking surface

Following the macroscopic investigations, it is observed that the rupture of the centromedullary stem occurred at the distal locking system and at this level of investigation no scratches are observed on the implant surface (which could be made at the time of insertion in the human body) or excessive friction. screw (figure 4.26).

FIG. 4.26 Overview of the rod

Figure 4.41 shows stereomicroscopy images taken on the breaking surface of the two components that form the rod.

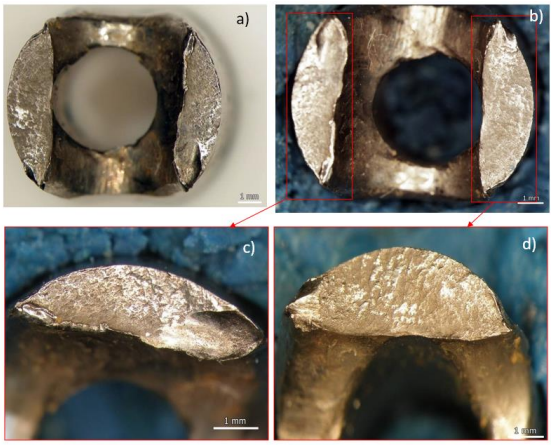

FIG. 4.27. Fractographic images of the breaking surface a) overview of the breaking area of the first part b) overview of the breaking area of the other part; c, d) details of the breaking surface associated with figure b)

For a more rigorous characterization of the explanted rod, microstructural investigations were performed. Thus, in figure 4.28 a, b) the biphasic structure α + β is highlighted which has a pattern similar to that of a fabric and consists of the lamellar distributed α phase and the β phase .

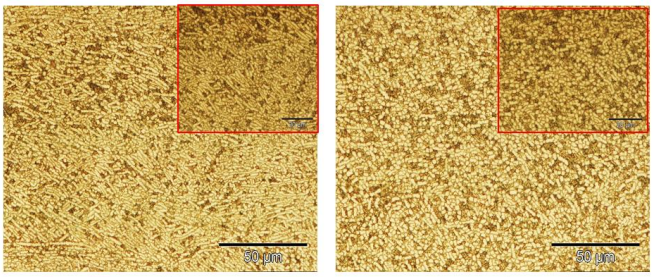

FIG. 4.28. MO images of the centromedullary rod (TCT4 test); a) the central area of the sample b) the area with a smaller thickness of the sample

In order to substantiate the phenomena / modes of rupture that took place in the case of the centromedullary rod-type explant, investigations were performed on the representative surfaces previously presented using the SEM method.

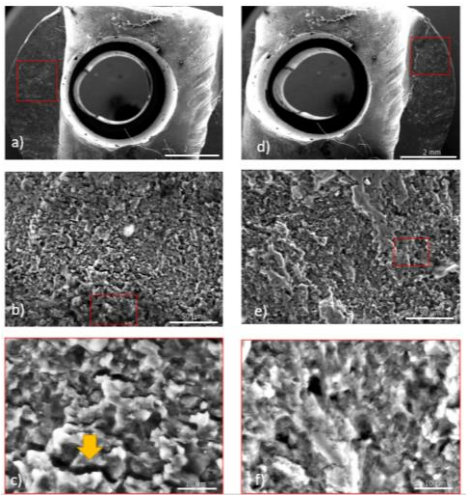

FIG. 4.29 SEM images of the breaking surface a) overall picture of the breaking surface (from the left of the hole); b) detail associated with the area marked in figure a); c) detail associated with the area marked in figure b); d) overview of the breaking surface (from the right of the hole); e) detail associated with the area marked in figure d); f) detail associated with the area marked in figure e)

4.2.5 TCT5 test

4.2.5.1. Clinical data

Table 4.11 presents the clinical data of the patient according to the established protocol, and Figure 4.30 presents images of bone fracture obtained by conventional radiology.

Table 4.11 Clinical patient data

PATIENT (*name, surname, age, sex*)	RM 67 years, F.
INTERNAL DIAGNOSIS	Post -fracture status calf operated in the 3 years ago . Callus tibial vices. Osteosynthesis material damaged .
CLINICAL OBSERVATION SHEET (*number*)	-
DATE and HOSPITAL in which the ***implantation was performed***	2015; another service
DATE and HOSPITAL in which the ***explant was performed***	2018, SCUB Floreasca
THE REASON FOR EXPLANING THE MEDICAL DEVICE	nonunion tight , relatively unstable with micro-movements in the outbreak that led in the time to damage osteosynthesis material _
IDENTIFICATION OF THE EXPLANTED DEVICE (* *type and components*)	Rod intramedullary tibial titanium ; Screw 4.5mm latch ;
DEVICE DATA (* *batch and device serial number, manufacturer)*	**C***

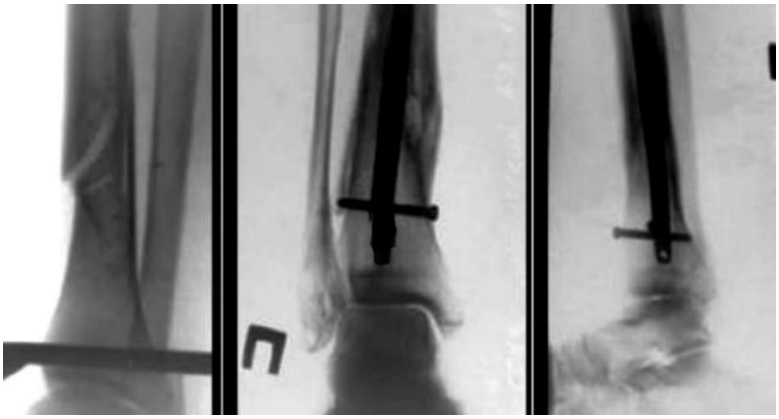

FIG. 4.31. Preoperative radiography - postoperative control with failure more than 2 years after implantation.

4.2.5.2 Investigations into: determination of chemical composition, assessment of chemical conformity and estimation of compositional homogeneity

4.2.5.2.a) Measurement of local chemical composition

The evaluation of the chemical homogeneity of the explanted tibial centromedullary stem was performed at the level of the test piece (sample), at which level the chemical homogeneity test is considered to be of the "in-bottle" type. Following the application of the t-Student test, it was found that the sample satisfies the homogeneity criteria for all identified elements, respectively C, Al, Cr, Mo, Fe, Si, Sn.

4.2.5.2.b) Chemical conformity assessment

The chemical conformity assessment was performed both in detail taking into account the results of the measurements locally and globally (synthetically) using the mean of the averages ($\bar{\bar{c}}$)and the uncertainty of the mean of the averages) ($U_{\bar{\bar{c}}}$).

Table 4.12 . Overall results of the chemical conformity test (CC) corresponding to the TCT5 sample

Item [%]	C	N	Fe	V	the	-R	Mo	Sn	And
LS [1] **	max 0.08	max0.05	max0.30	4.5	6.75	-	-	-	-
LI [2] **	-	-	-	3.5	5.5	-	-	-	-
$\bar{\bar{c}}$	0.043	-	0.273	-	5.95	**1.80**	**2.70**	**0.92**	**0.48**
U [95%]	0.002	-	0.01	-	0.04	**0.01**	**0.01**	**0.01**	**0.03**
LSB [3]	0.078	-	0.29	-	6.71	-	-	-	-
LIB [3]	-	-	-	-	5.46	-	-	-	-
TCC [4]	**1**		**1**	**0**	**1**				

1 Upper limit; 2 Lower limit; 3 Acceptance tape; 4 the result of the chemical conformity test

Following the assessment of the chemical conformity of the centromedullary rod locally and globally, it can be stated on the basis of the results obtained that the alloy **is not compliant .** In terms of concentrations .

4.2.5.3. Macroscopic analysis and microscopy tests (MO and SEM) to investigate the explant in terms of macrostructure, microstructure and morphology of the breaking surface

The explant investigation was performed according to the scheme implemented respectively from the point of view of macrostructure, microstructure and morphology of the breaking surface.

Figure 4.32 shows the overall image of the centromedullary rod.

FIG. 4.32 Overview of the centromedullary rod

The investigation of the centromedullary stem at macroscopic level reveals the place where the rupture occurred at the proximal locking system and at this level of investigation there are scratches on the implant surface due to the screw mobilized in the hole and which could be made at the time of insertion in the human body. be observed in the area indicated in figure 4.33).

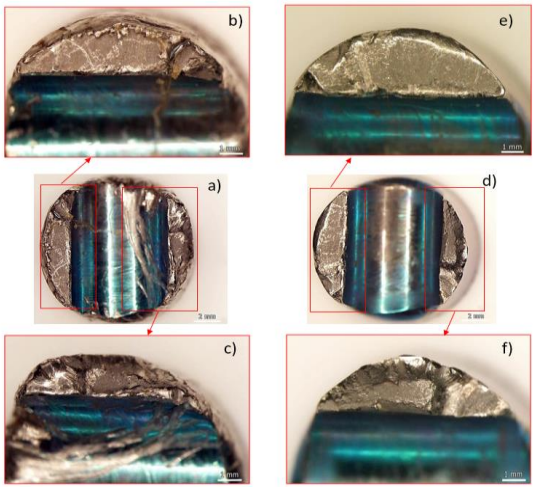

FIG. 4.33 Fractographic images of the fracture surfaces a) overview of the fracture area of the first part c, d) details of the fracture surface associated with figure a); d) overview of the breaking area of the other part; e, f) details of the breaking surface associated with figure d)

Figure 4.33 a, c shows surface aspects specific to excessive friction caused by the screw that was mobilized in the hole.

Optical microscopy investigations highlight a typical structure of the titanium alloy and a biphasic structure $\alpha + \beta$ as can be seen in Figure 4.34 a, b.

.

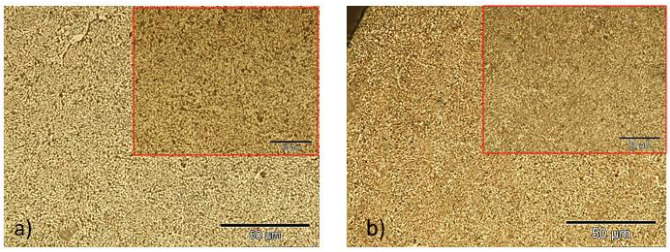

FIG. 4.34. MO images of the centromedullary rod a) central area of the sample b) marginal area of the sample

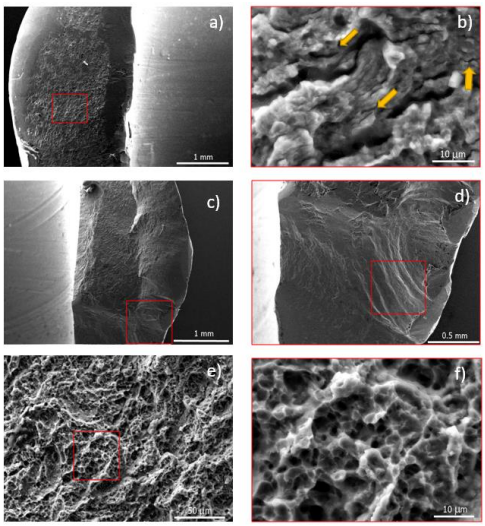

FIG . 4.35 SEM images of the breaking surface a) overall picture of the breaking surface (from the left of the hole); b) detail associated with the area marked in figure a); c) overview of the breaking surface (from the right of the hole); d) detail associated with the area marked in figure b); e) detail associated with the area marked in figure d); f) detail associated with the area marked in figure e)

overall images of the breaking surfaces (figure 4.35 a, c) show areas on the one hand extensive presenting _ issues crystalline-bright (central area) on the other areas relative smooth , glossy.

Performing stereomicroscopy, light microscopy and scanning electron microscopy analyzes eliminated the following possible causes of rupture, respectively: imperfections in the preparation and processing of materials.

The rupture area is located at the distal locking system, with clear traces of excessive friction of the screw and small scratches on the surface of the implant made at the time of insertion in the human body.

After a careful analysis of the clinical data, no uncorrelations were identified between the design of the exploded centromedullary rod and the type of condition in which it was used.

The rupture can be attributed to the high mechanical stress of the centromedullary rod which led to excessive friction of the screw mobilized in the hole and material fatigue.

4.2.6 TCF6 test

4.2.6.1. Clinical data on the implanted patient

Table 4.13 presents the patient's clinical data according to the established protocol, and Figure 4.36 presents images of bone fracture obtained by conventional radiology.

Table 4.13 Clinical patient data

PATIENT (*name, surname, age, sex*)	AC 56 years, M
INTERNAL DIAGNOSIS	Post -fracture status commutative operated femur . Pseudarthrosis right femur . Osteosynthesis material damaged .
CLINICAL OBSERVATION SHEET (*number*)	-
DATE and HOSPITAL in which the ***implantation was performed***	2017; another service
DATE and HOSPITAL in which the ***explant was performed***	2019, SUUB
THE REASON FOR EXPLANING THE MEDICAL DEVICE	Pseudoarthrosis with damage osteosynthesis material about 18 months after implantation initial , with resumption _ activity body rule
IDENTIFICATION OF THE EXPLANTED DEVICE (* *type and components*)	Rod centromedullary femur, universal , for application through bore , diameter 11 mm, titanium
DEVICE DATA (* *batch and device serial number, manufacturer)*	**C***
REMARKS	After an evolution gusset initial good - failure through fatigue

FIG. 4.37. Radiographs of the implanted area a, b) preoperative c, d postoperative

4.2.6.2. Investigations into: determination of chemical composition, assessment of chemical conformity and estimation of compositional homogeneity

4.2.6.2. a) measuring the local chemical composition

The evaluation of the chemical homogeneity of the exploded centromedullary rod was performed at the level of the test piece (sample), level at which the chemical homogeneity test is considered to be of the "in-bottle" type.

The reporting of the obtained results was performed in accordance with the values of the concentrations of the elements specified in the ISO 5832-3: 2016 standard.

4.2.6.2.b) Chemical conformity assessment

The chemical conformity assessment was performed both in detail taking into account the results of measurements locally and globally (synthetically) using the mean of the averages ($\bar{\bar{c}}$)and the uncertainty of the mean of the averages ($U_{\bar{\bar{c}}}$). The results of the conformity test are presented in the following table.

Table 4.14 . Overall results of the chemical conformity test (CC) corresponding to the TCF6 sample

Item [%]	C	N	Fe	V	the
LS [1] **	max 0.08	max0.05	max0.30	4.5	6.75
LI [2] **	-	-	-	3.5	5.5
$\bar{c}$	0.028	0.038	0.188	4.27	6.29
U [95%]	0.004	0.002	0.004	0.02	0.02
LSB [3]	0.076	0.298	0.296	4.48	6.73
LIB [3]	-	-	-	3.48	5.48
TCC [4]	**1**	**1**	**1**	**1**	**1**

1 Upper limit; 2 Lower limit; 3 Acceptance tape; 4 the result of the chemical conformity test

Following the chemical conformity assessment of the rod at local and global level, it can be stated based on the results obtained that the alloy **is compliant .** Regarding the concentrations of the elements as shown in table 4.122. Thus, the alloy subjected to the measurement corresponds to the predicted mark respectively Ti-6Al-4V .

4.2.6.3. Macroscopic analysis and microscopy tests (MO and SEM) to investigate the explant in terms of macrostructure, microstructure and morphology of the breaking surface

The explant was investigated according to the scheme implemented, respectively from the point of view of the chemical composition, macrostructure, microstructure and morphology of the breaking surface.

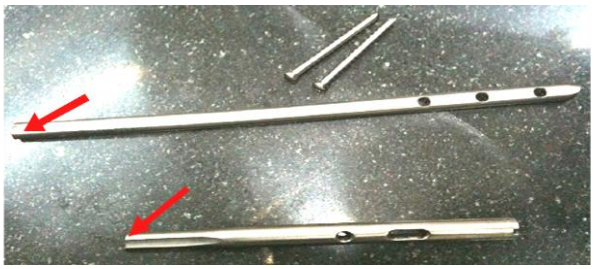

FIG. 4.38 Overview of the locked centromedullary rod

The investigation of the centromedullary stem at macroscopic level reveals the place where the respective rupture occurred in the middle area and at this level of investigation no scratches are observed on the implant surface.

In the following are presented stereomicroscopy images of the rupture surfaces in order to identify the causes that caused the implant failure (figure 4.39).

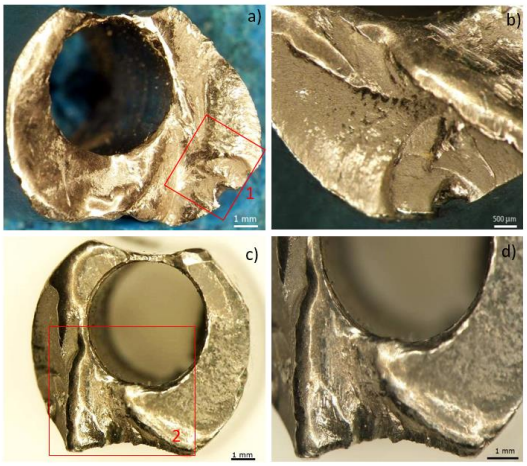

FIG. 4.39. Fractographic images of the breaking surfaces a) overview of the breaking area -1-; b) details of the breaking surface associated with figure a); c) overview of the breaking zone -2; d) details of the breaking surface associated with figure c)

Optical microscopy investigations highlight a typical structure of the titanium alloy in the Ti-Al-V system (Ti6Al4V), respectively a biphasic structure $\alpha + \beta$ as can be seen in Figure 4.40 a, b.

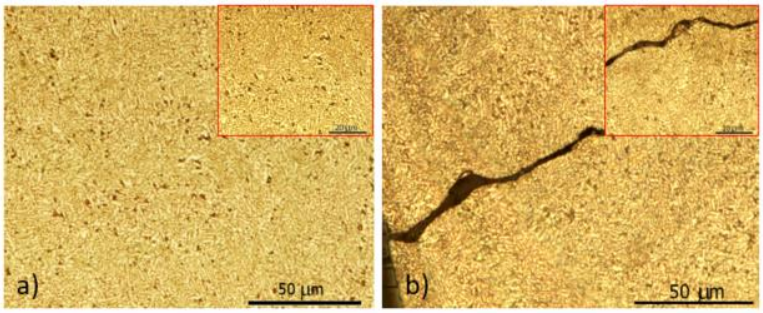

FIG. 4.40. MO images of the locked centromedullary rod (TCF6 test); a) the central area of the sample; b) the marginal area of the sample .

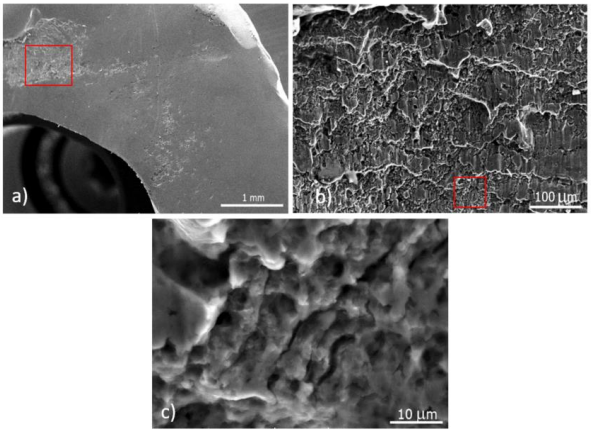

FIG. 4.41 SEM images of the breaking surface a) image of a portion of the breaking surface; b) detail associated with the area marked in figure a); c) detail associated with the area marked in figure b)

The image of an area of the fracture surface (figure 4.41 a) reveals a fracture with a complex character which in proportion of 90% has a fragile fracture aspect and an area with a mixed morphological aspect, respectively ductile-fragile. In figure 4.41 b) the mixed breaking character can be observed and the presence of dimples that alternate with the ductile breaking zones is highlighted

4.2.7 TCF7 test

4.2.7.1. Clinical data on the implanted patient

Table 4.15 presents the patient's clinical data according to the established protocol, and Figure 4.42 presents images of bone fracture obtained by conventional radiology.

Table 4.15 Clinical patient data

PATIENT (*name, surname, age, sex*)	DN 58 years old, M.
INTERNAL DIAGNOSIS	Post -fracture status supracondylar left femur operated in the 1 year ago . Pseudarthrosis right femur . Osteosynthesis material damaged .
CLINICAL OBSERVATION SHEET (*number*)	-
DATE and HOSPITAL in which the ***implantation was performed***	2017 other service
DATE and HOSPITAL in which the ***explant was performed***	2018, SCUB Floreasca
THE REASON FOR EXPLANING THE MEDICAL DEVICE	Pseudarthrosis with damage osteosynthesis material _

The area in which the centromedullary stem was implanted was investigated by radiography

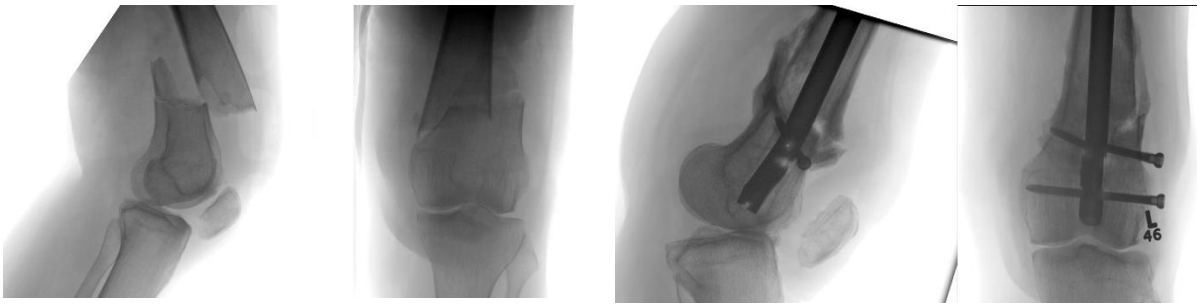

FIG. 4.43. Radiographs of the implanted area a, b) preoperative, c, d) at the date of revision

4.2.7.2. Investigations into: determination of chemical composition, assessment of chemical conformity and estimation of compositional homogeneity

4.2.7.2.a) measurement of the local chemical composition

The evaluation of the chemical homogeneity of the TCF7 sample was performed at the level of the test piece (sample), at which level the chemical homogeneity test is considered to be of the "in-bottle" type. Thus, for the evaluation of chemical homogeneity, the t-Student statistical test was applied using the experimental standard deviation of the means.

Following the application of the t-Student test, it was found that the sample does not meet the criteria of chemical homogeneity in the case of the elements Mn and N. For the other elements (S, Cr, Ni, Mo, Cu, Si) the sample satisfies the conditions of chemical homogeneity.

4.2.7.2.b) Chemical conformity assessment

The chemical conformity assessment was performed both in detail taking into account the results of measurements locally and globally (synthetically) using the mean of the averages ($\bar{\bar{c}}$)and the uncertainty of the mean of the averages $U_{\bar{\bar{c}}}$).

Table 4.16 . Global chemical conformity (CC) test results corresponding to TCF7 sample

Item [%]	C	And	min	P	S	-R	us	Mo	N	With
LS [1]	max 0.030	max 1.0	max 2.0	max0.025	max0.1	19.0	15.0	3.5	max 0.10	max 0.50
LI [2]	-	-	-	-	-	17.0	13.0	2.25	-	-
$\bar{C}_m$	0.023	0.341	2.08	0.013	0.018	17.08	14.15	2.83	0.192	0.049
U [95%]	0.002	0.016	0.04	0.002	0.004	0.10	0.10	0.02	0.004	0.003
LSB [3]	0.028	0.984	1.96	0.023	0.096	18.9	14.90	3.48	0.096	0.497
LIB [3]	-	-	-	-	-	17.1	13.10	2.29	-	-
TCC [4]	**1**	**1**	**0**	**1**	**1**	**1**	**1**	**1**	**0**	**1**

1 Upper limit; 2 Lower limit; 3 Acceptance tape; 4 the result of the chemical conformity test

Following the assessment of chemical homogeneity, the elements Mn and N do not satisfy the conditions of homogeneity. It can also be seen in Table 4.16 that N and Mn do not meet the requirements for compliance with the brand specification.

Following the assessment of the chemical conformity of the rod at local and global level, it can be stated on the basis of the results obtained that the rod is not compliant in terms of concentrations of the respective elements Mn and even more so if extended measurement uncertainties are taken into account (U [95 %]).

In conclusion , the sample to be measured corresponds to the predicted mark respectively 316L but **does NOT** comply with the ISO 5832-1 standard.

4.2.7.3. Macroscopic analysis and microscopy tests (MO and SEM) to investigate the explant in terms of macrostructure, microstructure and morphology of the breaking surface

The explant was investigated according to the scheme implemented, respectively from the point of view of the chemical composition, macrostructure, microstructure and morphology of the breaking surface.

Figure 4.44 shows the overall image of the centromedullary rod

F fig. 4.44 TCF7 sample overview

The investigation of the centromedullary stem at macroscopic level reveals the place where the respective rupture occurred in the middle area and at this level of investigation no scratches are observed on the implant surface.

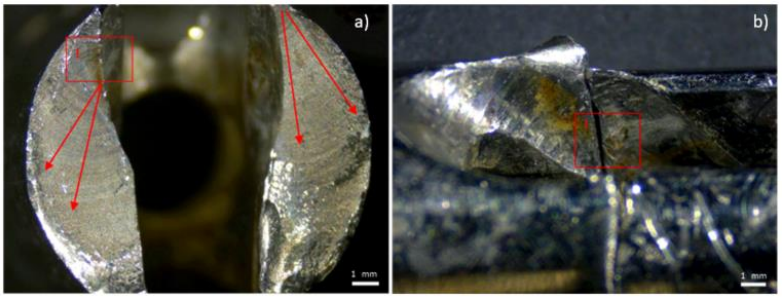

FIG. 4.45 Fractographic images of the breaking surface a) overview of the breaking area; b) details of the breaking surface associated with figure a);

The investigation of the breaking surface led to the identification of the breaking primer highlighted in the area marked in red. Figure 4.46 shows optical microscopy images of the resulting sample.

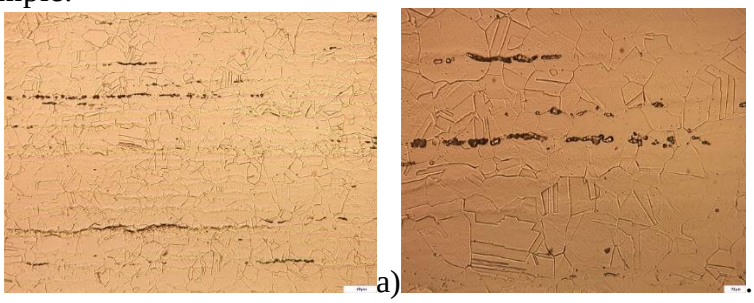

a) . b)

FIG. 4.46 MO images of the locked centromedullary rod (TCF7 test); a, b)

Optical microscopy images show a typical microstructure of plastically deformed stainless austenitic steel, with polyhedral and twinned grains

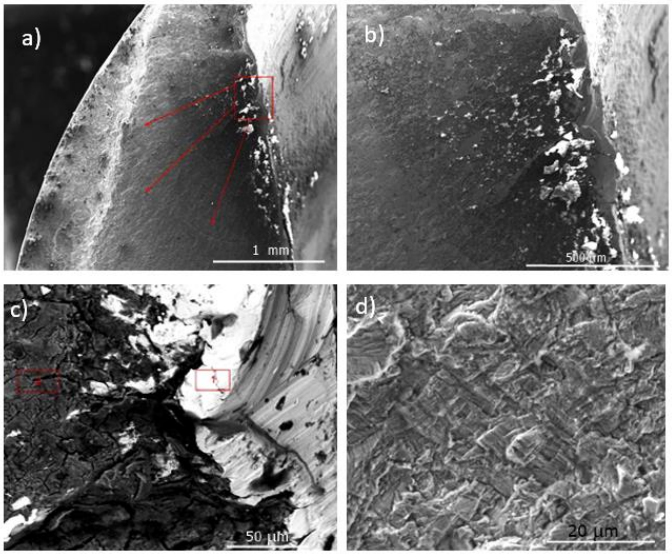

FIG. 4.47 SEM images of the breaking surface a) image of a portion of the breaking surface; b) detail associated with the area marked in figure a); c) detail associated with the area marked in figure b); d) detail associated with the area marked in figure c)

The image of the portion of the rupture surface (figure 4.47 a) reveals a rupture by cleavage. In one of the investigations of the rupture surface of the implant, it can be concluded that its rupture has a predominantly ductile character, in the area under discussion.

CHAPTER 5 - CONCLUSIONS

5.1 General conclusions

A pertinent analysis leading to progress in the field of implants requires a process of scientific research of the behavior of the studied implants. In this sense, scientific research must be understood as knowledge based on indisputable data and observations, empirically and or theoretically grounded in a non-combatable way.

The investigations of Stereomicroscopy, MO and SEM highlight the microstructure, the morphology of the breaking surfaces and implicitly of the breaking mechanism that takes place. SDAR-OES investigations provide data on the chemical composition of implants and can be used to estimate chemical homogeneity locally and globally by applying the t-Student test. Also, based on these investigations corroborated with the standards in force, the chemical conformity of the implants can be assessed. Therefore, following the studies performed on the selected samples, the following were identified:The PS1 sample satisfies the requirements of chemical homogeneity; and following the evaluation of the chemical conformity taking into account the extended uncertainty, it can be stated that the sample corresponds to the predicted mark, respectively Ti cp2.

- PS1-screw test screw meets the requirements of compliance with the respective brand specification Ti-6Al-V. It can be seen that the PS1-plate and PS1-screw sample are part of two different categories of material that could have theoretically led to the occurrence of galvanic corrosion phenomena, but it is considered that the interval in which the implant was in the body (3 months) it was not large enough and so no corrosion phenomena were observed on the surface of the plate or screws.
- The PS2 sample satisfies the requirements of chemical homogeneity and, following the assessment of local and global chemical conformity, it can be stated on the basis of the results obtained that it is compliant with regard to element concentrations and whether extended measurement uncertainties are taken into account. %)) it can be stated that the alloy subjected to the measurement corresponds to the predicted mark.

- The TCS3 sample does not meet the chemical homogeneity requirements for the elements Cu, Si, C, and Cu. However, following the assessment of chemical conformity at local and global level, it can be stated on the basis of the results obtained that the TCS3 sample is compliant in terms of element concentrations and if extended measurement uncertainties (U [95%]) are taken into account. It falls within the specified limits. The sample corresponds to the predicted mark respectively 316L.
- The TCT4 sample satisfies the homogeneity criteria for all the identified elements, respectively C, Al, Cr, Mo, Fe, Si, Sn. Following the assessment of chemical conformity at local and global level, it can be stated on the basis of the results obtained that the alloy is not compliant in terms of element concentrations as shown in Table 4.76. Thus, the sample does NOT correspond to the predicted brand, respectively Ti-6Al-4V [151]. Also, no type of biocompatible alloy could be identified that is similar to the investigated alloy. On the other hand, a similar alloy identified in ** GOST 19807/91 was identified, as shown in Table 4.77, an alloy used in the construction of submarines in the Russian Federation [156]. Thus, the exploded rod can be considered a non-biocompatible artifact, at the level of current information available. This may justify the improper behavior of the implant and is an obvious case of malpractice!

Following the reassessment of the chemical conformity, it is noted that the alloy from which the centromedullary rod was produced corresponds to the material class VT3-1 (BT3-1) from the GOST standard 19807/91 [156].

Based on the chemical conformity assessments in two situations respectively, in relation to ISO 5832-2 and in relation to GOST 19807/91 it is indubitable that the alloy belongs to class VT3-1. It should also be noted that the ISO 5832 standard does not specify that this alloy can be used in implantable products and this is a problem!

- The TCT5 sample satisfies the homogeneity criteria for all the identified elements, respectively C, Al, Cr, Mo, Fe, Si, Sn. Following the assessment of chemical conformity at local and global level, it can be stated based on the results obtained that the alloy is not compliant in terms of element concentrations as shown in Table 4.99. Thus, the alloy under measurement does NOT correspond to the predicted mark respectively Ti-6Al-4V.

- The TCF6 sample meets the homogeneity criteria for all elements specified in the standard. Following the assessment of the chemical conformity of the rod at local and global level, it can be stated based on the results obtained that the alloy is compliant in terms of element concentrations as shown in Table 4.122. Thus, the alloy subjected to the measurement corresponds to the predicted mark respectively Ti-6Al-4VThe TCF7 sample does not meet the criteria of chemical homogeneity in the case of Mn and N elements. Also, following the local and global chemical conformity, it can be stated based on the obtained results that the sample does not comply with all the more so if the extended measurement uncertainties (U [95%]) are taken into account. The sample to be measured corresponds to the predicted mark respectively 316L but does NOT comply with the ISO 5832 standard.

The results of the tests performed on the investigated samples support the following statement: there are medical devices on the market that do NOT meet the requirements of ISO 5832, ISO 13485: 2016 / Rev.2020, which is a problem and a threat to the quality of human life.

Following the MO, all the investigated samples present microstructures characteristic of the respective investigated material: the PS1 and PS2 samples have a microstructure characteristic of non-alloyed titanium; TCS3, TCF7 have a microstructure characteristic of a stainless steel, and samples TCT4, TCT5, TCF6 have a biphasic structure characteristic of a titanium alloy.

Stereomicroscopy and SEM investigations on the rupture surfaces revealed the following: structural homogeneities in the rupture area, which leads to fracture due to external factors; in the second case, morphological aspects specific to the cleavage are revealed, in the direction of the local fissure; the third test shows traces caused by the instrument used by the

doctor during the implant removal maneuver; also, the fourth sample shows signs of wear; in the case of the fifth sample, the surface morphology presents characteristic aspects of a ductile fracture, respectively, can be distinguished morphologies of the cup type of unequal sizes, the rupture highlights surface aspects specific to excessive friction caused by the screw that was mobilized in the hole; in the case of the sixth test, the surface morphology presents characteristic aspects of both ductile and fragile rupture, so it can be concluded that its rupture is dual and ductile-fragile, stereomicroscopic investigations highlighting the existence of a technical manufacturing defect proven by the eccentricity of the hole interiors; the seventh sample, the breaking surface presents morphological aspects characteristic of the material fatigue, with endogenous inclusions distributed unevenly, and the probability of occurrence of the rod cracking becomes very high.

5.2. **Personal and original contributions**

Improving mechanical characteristics and product design in terms of performance / cost is a field of research in continuous development in which a wide variety of materials can be researched to improve the quality of human life and the field of biomaterials.

1. Design of the protocol for explanting medicated devices to investigate and establish the causes of implant failure concerning: clinical data, available information on the material used and methods and techniques used to identify the causes that led to the implant failure

2. Application of the method for estimating the uncertainty of the measurement of elemental concentrations with SDAR-OES equipment.

3. Application of the method of analysis of chemical homogeneity by the t-Student test to estimate the chemical homogeneity of explants.

4. Assessment of the chemical conformity of explants that can be extended to any type of biomaterial and that from the results obtained is imperative to be performed on any metallic material that meets (or is declared to meet) the biocompatibility criteria.

5. Case studies performed on a number of 7 explants As a result of which it was found the importance of using the selected investigation methods

6. Highlighting the problem of screws In the case of both types of implants, respectively in the case of the plate, the screws corrode (corrosion in the crevasse and have a ductile rupture, usually)

7. Imposing the verification of the quality (conformity) of the osteosynthesis material. Based on the results obtained, it was found that sometimes the materials used are not taken into account îtogether together plate-screw, rod-screw (theoretically they have the same chemical composition, practically, they are different), and even more so non-conformities of the chemical composition were identified which does not comply with the requirements of the specific standards for that material.

5.3. **Perspectives for further development**

Following the studies performed on the selected samples and the results obtained (presented in this thesis) we identified the following future directions of research / development in the topic of the thesis:

Research to improve plaque implants by plugging holes that do not use screws. One solution would be to use a plug for unused holes

- The most important result of the thesis is to discover the non-conformity of the implants that should be reported.
- The need for additional research to confirm or deny that the modification / adjustment of the design of plate implants brings improvements in their performance.
- Wide application of the implemented protocol of implants especially in terms of chemical homogeneity and assessment of chemical conformity before their use !!

- New technical solutions for improving the functional performance of implants, respectively Replacing screws with plugs or cut-off screws or resorbable screws / Mg for plates
- New technical solutions to improve implantation techniques (guided insertion of screws in centromedullary rods)
- Simulations / simulation program aintebefore implant selection (also take into account material not only AO / medical criteria)

SELECTIVE REFERENCES

[1] R. M. Malina, C. Bouchard, Oded Bar-Or, Growth, Maturation, and Physical Activity, Cap.6 Bone tissue in skeletal growth and body composition, Ed. Human Kinetics, 2004
[2] F. F. Safadi, M. F. Barbe, S. M. Abdelmagid, M. C. Rico, R. A. Aswad, J. Litvin, and S. N. Popoff, Chapter 1- Bone Structure, Development and Bone Biology, Ed. Humana Press, 2009, pag. 1-50;
[3] R. Karpiński , Ł. Jaworski, P. Czubacka, The structural and mechanical properties of the bone, Journal of Technology and Exploitation in Mechanical Engineering Vol. 3, no. 1, 2017
[4] Hanawa, T. (2019). Titanium–Tissue Interface Reaction and Its Control With Surface Treatment. Frontiers in Bioengineering and Biotechnology, 7:170
[5] Karl-Heinz Frosch, Klaus Michael Stürmer, Metallic Biomaterials in Skeletal Repair, Eur J Trau ma 2006;32:149–59
[6] Ghosh, S., Sanghavi, S., & Sancheti, P. Metallic biomaterial for bone support and replacement. Fundamental Biomaterials: Metals, 2018, pp. 139-165.
[7] Sepideh Kamrani . Claudia Fleck, Biodegradable magnesium alloys as temporary orthopaedic implants: a review, Biometals Vol. 32, 2019, pp. 185–193
[8] Antoniac I; Laptoiu D; Blajan AI; Cotrut C; Instrumentar si dispozitive chirurgicale, Editura Printech, Bucuresti, 2011
[9] M. Bane, I. Ciucă, Cap.8, Tratat de ştiinţa şi ingineria materialelor metalice,Vol I, Editura Agir, 2006, pag. 1103-1114
[10] N. Popescu, R. Şaban, D. Bunea, I. Pencea, Ştiinţa materialelor pentru ingineria mecanică , Vol 1, , Ed.Fair Partners, 1999, pag 74-81
[11]. I. Pencea, Capitol 8, Metode și tehnici instrumentale de analiză elementală a materialelor, p.1085-1099, Tratat de știința și Ingineria materialelor metalice, vol.5, Editura Agir, București, 2011
[11]. I. Pencea, Bazele încercărilor spectrochimice de emisie optică prin scânteie şi arc electric, Ed. Printech, 2007, pag. 190-203
[12] M. Branzei, D. Gheorghe, I. Ciuca, Capitol 8, Microscopie optica calitativă și cantitativă, p.1019-1038, Tratat de știința și Ingineria materialelor metalice, vol.5, Editura Agir, București, 2011
[13] Silviu Butnariu, Gheorghe Mogan, Analiza cu elemente finite în ingineria mecanică, Ed. Univ. Transilvania din Brașov, 2014
[14] ***, ANSYS Structural Analysis Guide, ANSYS Inc., SAS IP, 2004.
[141] *** SR Ghid ISO 98-3/2010, Incertitudine de măsurare. Partea 3 : Ghid pentru exprimarea incertitudinii de măsurare
[15] C.E. Sfat, C.E. Serban, Capitol 8, Asigurarea calităţii rezultatelor încercărilor, p.1272-1276, Tratat de știința și Ingineria materialelor metalice, vol.5, Editura Agir, București, 2011
[16] ISO 5832-2 ISO 5832-2:2018 Implants for surgery — Metallic materials — Part 2: Unalloyed titanium
[17] *** ISO 5832-3:2016 Implants for surgery — Metallic materials — Part 3: Wrought titanium 6-aluminium 4-vanadium alloy
[18] I. V. Antoniac, D. I. Stoia, B. Ghiban, C. Tecu, F. Miculescu, C. Vigaru, V. Saceleanu, Failure Analysis of a Humeral Shaft Locking Compression Plate—Surface Investigation and Simulation by Finite Element Method, Materials 2019, 12, 1128

Content

INTRODUCTION 3

CHAPTER 1. MEDICAL CLINICAL ASPECTS 3

1.1. GENERAL CONSIDERATIONS 3

2.1. FUNDAMENTALS OF THE BONE PROTESION APPROACH 3

2.2. CURRENT STATE OF METAL BIOMATERIALS 4
2.2.1.1. The current state of stainless steels 4
2.2.1.2. Current status of titanium and titanium alloys 4

2.2.1.3. The current state of magnesium alloys 4

2.2.2 Types of implants for osteosynthesis 4

CHAPTER 3 RESEARCH METHOD 5

3.1. The purpose of the doctoral thesis 5

3.2. The objectives of the doctoral thesis 5

CHAPTER 4 EXPERIMENTAL RESULTS ON THE ANALYSIS OF METAL IMPLANT IMPLANTS FOR OSTEOSYNTHESIS 7

4.2. EXPERIMENTAL RESULTS 7

4.2.1. Sample PS1 7
4.2.1.2 a) Measurement of local chemical composition 8
4.2.1.2 b) Chemical conformity assessment 8
4.2.1.3. Macroscopic analysis and microscopy tests (MO and SEM) to investigate the explant in terms of macrostructure, microstructure and morphology of the breaking surface 9
4.2.1.4. Finite element analysis 11

4.2.2 PS2 test 12
4.2.2.1. Clinical data on the implanted patient 12
4.2.2.2. Investigations into: determination of chemical composition, assessment of chemical conformity and estimation of compositional homogeneity 13
4.2.2.2 a) Measurement of local chemical composition 13
4.2.2.2 b) Chemical conformity assessment 13
4.2.2.3. Macroscopic analysis and microscopy tests (MO and SEM) to investigate the explant in terms of macrostructure, microstructure and morphology of the breaking surface 14
4.2.2.4. Finite element analysis 15

TCS3 test 18
4.2.2.1. Clinical data on the implanted patient 18
4.2.3.1. Clinical data on the implanted patient 18
4.2.3.2. Investigations into: determination of chemical composition, assessment of chemical conformity and estimation of compositional homogeneity 19
4.2.3.2 a) Measurement of local chemical composition 19
4.2.3.2 b) Chemical conformity assessment 19
4.2.3.3. Macroscopic analysis and microscopy tests (MO and SEM-EDS) to investigate the explant in terms of macrostructure, microstructure and morphology of the fracture surface 20

4.2.4 TCT4 test 21
4.2.4.1. Clinical data on the implanted patient 21
4.2.4.2. Investigations into: determination of chemical composition, assessment of chemical conformity and estimation of compositional homogeneity 22
4.2.4.2.a) Measurement of local chemical composition 23
4.2.4.2.b) Chemical conformity assessment 23
4.2.4.3. Macroscopic analysis and microscopy tests (MO and SEM) to investigate the explant in terms of macrostructure, microstructure and morphology of the breaking surface 23

4.2.5 TCT5 test 25
4.2.5.1. Clinical data 25
4.2.5.2 Investigations into: determination of chemical composition, assessment of chemical conformity and estimation of compositional homogeneity 25
4.2.5.2.a) Measurement of local chemical composition 25
4.2.5.2.b) Chemical conformity assessment 26
4.2.5.3. Macroscopic analysis and microscopy tests (MO and SEM) to investigate the explant in terms of macrostructure, microstructure and morphology of the breaking surface 26
4.2.6 TCF6 test 28
4.2.6.1. Clinical data on the implanted patient 28
4.2.6.2. Investigations into: determination of chemical composition, assessment of chemical conformity and estimation of compositional homogeneity 29
4.2.6.2. a) measuring the local chemical composition 29
4.2.6.2.b) Chemical conformity assessment 29
4.2.6.3. Macroscopic analysis and microscopy tests (MO and SEM) to investigate the explant in terms of macrostructure, microstructure and morphology of the breaking surface 29
4.2.7 TCF7 test 31
4.2.7.1. Clinical data on the implanted patient 31
4.2.7.2. Investigations into: determination of chemical composition, assessment of chemical conformity and estimation of compositional homogeneity 32
4.2.7.2.a) measurement of the local chemical composition 32
4.2.7.2.b) Chemical conformity assessment 32
4.2.7.3. Macroscopic analysis and microscopy tests (MO and SEM) to investigate the explant in terms of macrostructure, microstructure and morphology of the breaking surface 32

5.1 General conclusions 34

5.2. Personal and original contributions 36

5.3. Perspectives for further development 36

SELECTIVE REFERENCES 37